Manuscript submitted to
AIMS' Journals
Volume **X**, Number **0X**, XX **200X**

Website: http://AIMsciences.org

pp. **X–XX**

EFFECTIVE VISCOSITY OF BACTERIAL SUSPENSIONS: A THREE-DIMENSIONAL PDE MODEL WITH STOCHASTIC TORQUE

BRIAN M. HAINES, IGOR S. ARANSON, LEONID BERLYAND, AND DMITRY A. KARPEEV

Brian M. Haines

Department of Mathematics, Penn State University, McAllister Bldg.
University Park, PA 16802 USA

Igor S. Aranson

Materials Science Division, Argonne National Laboratory
9700 South Cass Avenue
Argonne, IL 60439 USA

Leonid Berlyand

Department of Mathematics, Penn State University, McAllister Bldg.
University Park, PA 16802 USA

Dmitry A. Karpeev

Mathematics and Computer Science Division, Argonne National Laboratory
9700 South Cass Avenue
Argonne, IL 60439 USA

(Communicated by the associate editor name)

Date: August 24, 2010.

2000 *Mathematics Subject Classification.* Primary: 92B99, 76A05, 35Q35.

Key words and phrases. Bacterial Suspensions, Effective Viscosity, Homogenization.

The work of I.S. Aranson was supported by the US DOE Office of Basic Energy Sciences, Division of Materals Science and Engineering, contract DE-AC02-06CH11357. The work of B. Haines and L. Berlyand was supported by the DOE grant DE-FG02-08ER25862 and NSF grant DMS-0708324.

Abstract. We present a PDE model for dilute suspensions of swimming bacteria in a three-dimensional Stokesian fluid. This model is used to calculate the statistically-stationary bulk deviatoric stress and effective viscosity of the suspension from the microscopic details of the interaction of an elongated body with the background flow. A bacterium is modeled as an impenetrable prolate spheroid with self-propulsion provided by a point force, which appears in the model as an inhomogeneous delta function in the PDE. The bacterium is also subject to a stochastic torque in order to model tumbling (random reorientation). Due to a bacterium's asymmetric shape, interactions with prescribed generic planar background flows, such as a pure straining or planar shear flow, cause the bacterium to preferentially align in certain directions. Due to the stochastic torque, the steady-state distribution of orientations is unique for a given background flow. Under this distribution of orientations, self-propulsion produces a reduction in the effective viscosity. For sufficiently weak background flows, the effect of self-propulsion on the effective viscosity dominates all other contributions, leading to an effective viscosity of the suspension that is lower than the viscosity of the ambient fluid. This is in qualitative agreement with recent experiments on suspensions of *Bacillus subtilis*.

1. **Introduction.** In this paper, we study the rheology of dilute suspensions of self-propelled swimming bacteria. Such suspensions are of particular interest because experimental observations show that the microscopic effect of bacterial self-propulsion leads to macroscopic phenomena. For example, experiments on bacteria suspended in liquid films have demonstrated enhanced diffusion of tracer particles [38], enhanced mixing [33], and collective flow speeds that exceed the speed of an individual bacterium by an order of magnitude [32]. Recently, in experiments reported in [31], activity (i.e., swimming) of *B. subtilis* was observed to cause a decrease in the effective viscosity of the suspenson by up to a factor of 7 compared to a suspension of inactive (dead) bacteria. These experimental results point to the potential for many technological applications (see [20]), but are not adequately explained by present theories.

Whereas phenomenological arguments relating the viscosity of suspensions to the activity of particles [13], simple kinetic models [29] and studies of viscosity in two-dimensional geometry [11] have been presented, the issue of viscosity in suspensions of swimmers still lacks conceptual clarity. In [13], a tensor order parameter $\mathbf{Q}$ is used to characterize the local ordering of the system (i.e., the alignment of swimming particles to each other). The governing dynamics for $\mathbf{Q}$ is borrowed from the theory of systems with nematic ordering and is phenomenological. In particular, the relationship of the evolution of the order paramter to the microscopic alignment dynamics has not been clarified, and the very possibility of arriving at macroscopic expressions for the effective viscosity from first-principle arguments has not been established. In this work we begin to fill this gap by proposing a model that allows for an analytic explanation of the observed effects.

Suspensions of swimming bacteria (or bacterial suspensions) are a prime example of *active suspensions*—suspensions in which the suspended particles or inclusions inject energy and momentum into the surrounding fluid, usually through self-propulsion. Bacteria come in a variety of shapes and employ many different forms of self-propulsion. We will only consider bacteria similar to the *B. subtilis* used in the experiments in [31, 32]. This is a rod-shaped unicellular microorganism with an aspect ratio of approximately 5.7 that propels itself through the motion of several helical flagella distributed over the surface of its body. These flagella are

driven by reversible molecular motors located inside the bacterial cell, which are in turn driven by electrochemical gradients across internal membranes (see [24]). The flagella allow a bacterium to move in two distinct modes: forward movement (swimming) and tumbling (random reorientation). The bacterium spends most of its time moving forward by bundling its flagella together so that they rotate as one strand, providing forward thrust (see Fig. 1). At random times the flagella unbundle and move separately (see Fig. 1), causing the bacterium to rotate (see e.g., [35, 30]) until the next bundling event. Depending on external conditions (e.g., the concentration of bacteria, the pH of the water, or the amount of nutrients and dissolved oxigen), the frequency and duration of tumbling events varies: the average time between events varies from 1 to 60 seconds and the average duration of tumbling is between 0.1 and 0.5 seconds (see [35]). This effectively results in an instant random reorientation of the bacterium. It has been observed in [37] and [36] that the process of tumbling makes bacterial motion in a fluid otherwise at rest similar to a three-dimensional random walk.

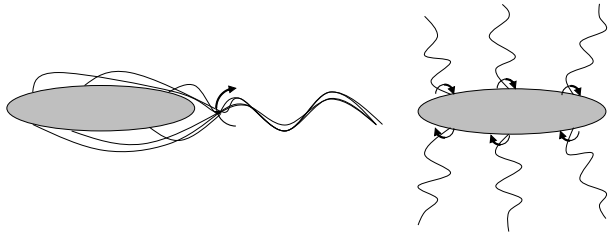

FIGURE 1. Diagram of a bacterium moving forward by bundling its flagella and rotating them together as one strand (left); Diagram of a bacterium tumbling by unbundling its flagella and rotating them independently (right).

The bulk properties of *passive* dilute suspensions (suspensions of inert particles, or inclusions) have been studied extensively for over 100 years. In 1905 Einstein studied the dilute limit when interparticle distances are much greater than the size of the particles themselves so that the volume fraction of the inclusions ϕ is a small parameter. He assumed that the effect of hydrodynamic interactions between the inclusions can be ignored in this case. He then calculated the linear correction in ϕ to the viscosity of the surrounding fluid due to the presence of neutrally buoyant, inert spheres (see [7]). In 1922, in [19], Jeffery attempted to do the same for ellipsoids, but found that the answer depended on the evolution of the distribution of orientations of inclusions, which he did not study. This work was not picked up again until Hinch and Leal produced a series of papers in the 1970s, most notably [22, 15], in which they studied the dynamics of ellipsoids in a shear flow and applied the results of this study to determining the effective viscosity of a suspension. In that work, the ellipsoids are subjected to rotational white noise, which drives the distribution of the orientations of inclusions to a unique steady state P^∞ irrespective of the initial distribution. Using P^∞, they then calculate the effective viscosities for various limiting cases of particle shape and shear strengths. In 1972, Batchelor and Green, in [2], were the first to consider pairwise particle interactions in order to find the $\mathcal{O}(\phi^2)$ correction to Einstein's result.

Up to this point, all works have involved *formal* asymptotics. In the 1980s, rigorous homogenization results were first proven for moderate concentrations of

particles in Stokesian fluids by Levy and Sanchez-Palencia in [23] and Nunan and Keller in [26]. Results for the densely-packed regime were more recently proven in 2007 in [3], [5], and [4]. A rigorous mathematical justification of Einstein's original formula for the effective viscosity of dilute passive suspensions has only recently been carried out in [10].

The history of the mathematical study of active suspensions is much shorter. Bacterial suspensions or suspensions of other swimming microorganisms have been the main vehicle of study of the macroscopic properties of active suspensions. Producing an adequate model for swimming bacteria has proved challenging. Numerical simulations in [16] using spherical swimmers with imposed body surface velocities modeling self-propulsion were able to predict a decrease in viscosity only in the presence of a gravitational field. This is because a bacterium acts as a force dipole (since the total force on the bacterium is zero: the force of self-propulsion is balanced by the viscous drag force), which will increase the viscosity when aligned in some directions (measured with respect to a principal axis of the background flow) and decrease it in others. For a rotationally symmetric particle, the lack of any preferred orientation will cause the active contributions to the viscosity to cancel and result in no change in the effective viscosity. Many other models have been presented, including some that including tumbling [27, 34], though these have not been used to study the effective viscosity.

In our previous work in [11], we modeled a bacterium as a disk in two dimensions with a point force directed radially outward from the body. An asymptotic formula, to first order in ϕ, was obtained for the effective viscosity of such a suspension given a prescribed orientation distribution function P. In that work, P was regarded as instantaneous and imposed. For distributions concentrated along the stable principal axis of the background flow, the asymptotic formula predicts a reduction in the effective viscosity relative to the case of passive disks. This can be understood heuristically: bacteria are force dipoles, and when a force dipole is aligned along the stable principal axis of a straining flow, it contributes to the bulk rate of strain. Thus, to maintain a constant rate of strain in the presence of dipoles aligned along this axis, the rate of work needed to be done on the boundary is decreased, which is equivalent to having a decreased effective viscosity. Concentration along this axis only occurs, however, for asymmetric particles.

In this paper, we provide the mathematical details of results presented in [12]. In this work, we significantly generalize and extend the work in [11]. We consider asymmetric bacteria in a three-dimensional geometry and include the effects of tumbling (random reorientation). We have derived analytical expressions for all components of the deviatoric stress tensor and explicit expressions for the effective viscosity in several relevant cases. The most significant aspect of this work is that instead of using a phenomenological theory of alignment, we use a microscopic model of self-propelled asymmetric bacteria in a Stokesian fluid as our departure point. Within this model we derive quantitative expressions for the statistically stationary probability distributions of orientations of bacteria, from which the mean bulk stress and the effective viscosity can be obtained in a straightforward manner. Our analysis shows a general trend of decreasing effective viscosity with increasing bacterial concentration and activity (speed of swimming). Furthermore, our results can be used to derive explicit evolution equations for the order parameter $\mathbf{Q}$ used in [13] and, hence, allow for a comparison with a phenomenological theory of nematic ordering.

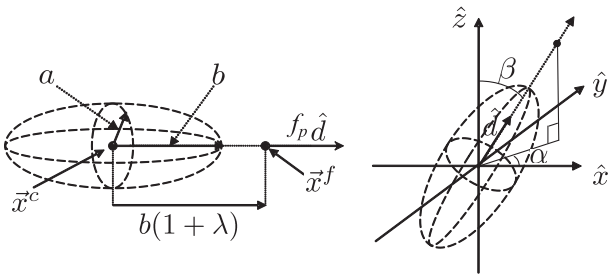

FIGURE 2. Diagram of a bacterium (left); A bacterium with orientation (α, β), alternatively described by the unit vector $\hat{d}$ (right).

We develop a PDE model with white noise that captures the effects of asymmetry, self-propulsion and tumbling. Following the work of Hinch and Leal in [15], we analyze the long-term dynamics of the particle distribution density governed by a Fokker-Plack equation. We emphasize this point, since dynamics has frequently been omitted from the previous analytical work, even on passive suspensions, due to the difficulties it presents. The presence of white noise is important because it ensures that the steady-state distribution of orientations of the bacteria (which the effective viscosity will depend on) is unique.

2. **Formulation.** We consider the motion of n neutrally buoyant bactera in a prescribed flow of the surrounding fluid in $\mathbb{R}^3$. In addition to being conveyed by the flow, the bacteria propel themselves by means of a rigidly attached point force (i.e., the location and orientation are fixed relative to the center of the body), which models the propulsion force caused by rotating helical flagella. In order to model tumbling, each bacterium exerts a random torque on the fluid. We select this torque in order to make its orientation in the absense of other effects (i.e., in a fluid at rest) a white noise process on the unit sphere.

During forward motion, the body of a bacterium rotates about its axis of symmetry in a direction opposing the rotation of its flagella in order to conserve angular momentum. However, since this rotation occurs about its axis of symmetry, its orientation is unaffected. Therefore, the only effect this rotation has on the effective viscosity is through the additional hydrodynamic stress it produces. Nevertheless, the Stokes flow due to a dipole decays as $1/r^2$ in 3D, while the flow due to the rotation of a torque-free rigid particle decays as $1/r^3$, so this rotation can be neglected.

Since we are primarily motivated by experimental results for *B. subtilis*, which are elongated (see illustration in Fig. 1), we model the lth bacterium as a prolate spheroid B^l with (arbitrary) eccentricity $e = \frac{\sqrt{b^2-a^2}}{b}$ (see Fig. 2). The orientation of the bacterium is specified by the angles (α^l, β^l) or, equivalently, by a unit vector $\hat{d}^l = (\cos\alpha^l \sin\beta^l, \sin\alpha^l \sin\beta^l, \cos\beta^l)$. Propulsion is modeled by a point force of magnitude f_p^l directed along $\hat{d}^l$ and applied at position $\vec{x}^{f,l}$ behind the bacterium on the major axis of the ellipsoid at a distance $(1+\lambda)\,b$ from its center $\vec{x}^{c,l}$ (see Fig. 2). We assume that, based on the size and propulsion force of the bacteria, the Reynolds number of the flows in the fluid surrounding the bacteria is small, so that inertial effects can be ignored and the fluid is Stokesian. Moreover, we assume that a steady-state flow is established on timescales much smaller than the typical timescale associated with bacterial movement (e.g., the time needed for a bacterium

to translate a significant fraction of its length or rotate by an appreciable angle). Therefore, we assume that the fluid surrounding the bacteria is governed by the steady Stokes equation.

The equations of motion of the bacteria are obtained by enforcing the balance of forces and torques. The motion of the bacteria themselves is assumed to be overdamped, ignoring inertial effects, so that the equations of motion contain no intertial terms. The fluid exerts hydrodynamic drag on the bacteria balancing the force of propulsion. Since the applied force is directed along the axis of the ellipsoid, it produces no torque. However, we add additional random torque τ selected to result in Gaussian white noise of the orientation vector $\hat{d}^l$ in the absence of other effects, in order to model tumbling. This random torque is balanced by that generated by hydrodynamic drag on the bacterium. We now formulate this in terms of a PDE problem.

Let $\vec{u}$ and p represent the velocity and pressure in the ambient fluid in $\Omega_F := \mathbb{R}^3 \setminus \cup_l B^l$, respectively, and η be the fluid's dynamic viscosity. The bacteria are submerged in a linear background flow $\vec{u}^b = E \cdot \vec{x} + \vec{\Omega} \times \vec{x}$ with the rate of strain tensor E (constant, symmetric, and trace-free matrix) and vorticity $\vec{\Omega}$ (constant vector). It is sufficient to consider only linear background flows since these determine the effective viscosity uniquely in terms of the orientations of the bacteria. The dynamics of the fluid in Ω_F and the motion of the bacteria are governed by

$$\begin{cases} \eta \Delta \vec{u} = \nabla p + \sum_l f_p^l \hat{d}^l \delta(\vec{x} - \vec{x}^{f,l}) & \vec{x} \in \Omega_F \\ \nabla \cdot \vec{u} = 0 & \vec{x} \in \Omega_F \\ \vec{u} = \vec{v}^l + \vec{\omega}^l \times \left(\vec{x} - \vec{x}^{c,l}\right) & \vec{x} \in \partial B^l \\ \vec{u} \to E \cdot \vec{x} + \vec{\Omega} \times \vec{x} & \vec{x} \to \infty \\ \int_{\partial B^l} \sigma \cdot \hat{\nu} dx + f_p^l \hat{d}^l = 0 & \\ \int_{\partial B^l} \sigma \cdot \hat{\nu} \times \left(\vec{x} - \vec{x}^{c,l}\right) dx + \vec{\tau}^l = 0, & \end{cases} \tag{1}$$

where $\hat{\nu}$ is the unit normal to the surface of integration and $\sigma_{ij} := -p\delta_{ij} + \eta\left(\frac{\partial u_i}{\partial x_j} + \frac{\partial u_j}{\partial x_i}\right)$ is the hydrodynamic stress tensor. The last two equations represent the balance of forces and torques and implicitly define the equations of motion of the bacteria. Namely, the linear and angular velocities $\vec{v}^l$ and $\vec{\omega}^l$, respectively, of the bacteria must be such that the balance conditions are satisfied. The choice of the random torque $\vec{\tau}^l$ is explained in Section 2.2. Note that all quantities are time-dependent, including the domain Ω_F, since the bacteria will tend to translate and rotate due to interaction with the background flow, self-propulsion, and rotational white noise.

Once the flow $(\vec{u}, p)$ has been calculated, one can calculate the *instantaneous* bulk deviatoric stress, defined by

$$\Sigma_{ij}^t(\vec{u}, p) := \frac{1}{|V|} \int_V \left(\sigma_{ij} - \frac{1}{3}\delta_{ij}\sigma_{kk}\right) dx, \tag{2}$$

where δ_{ij} is the Kronecker delta, V is any volume containing the entire suspension (the value of the integral is independent of this choice–see, e.g., [1]), and $|V|$ is the volume of V. An instantaneous effective viscosity $\hat{\eta}^t$ is then defined by choosing E and $\vec{\Omega}$ corresponding to a planar shear or pure straining flow of strength γ taken,

for concreteness, in the x, y plane:

$$E = \frac{1}{2}\begin{pmatrix} 0 & \gamma & 0 \\ \gamma & 0 & 0 \\ 0 & 0 & 0 \end{pmatrix} \tag{3}$$

with $\vec{\Omega} = \left(0, 0, \frac{\gamma}{2}\right)$ and $\vec{\Omega} = (0, 0, 0)$, respectively, and setting

$$\hat{\eta}^t(\vec{u},\, p) := \frac{\Sigma^t_{12}(\vec{u},\, p)}{\gamma}. \tag{4}$$

Here, we use γ in the denominator because this is the appropriate component of the bulk rate of strain. In principal, the effective viscosity should be a tensor of rank 4 with the quantity $\hat{\eta}^t$ above corresponding to the component $\hat{\eta}^t_{1212}$. Since we will calculate the bulk stress explicity, all components can easily be obtained by solving the linear system $\Sigma^t = E\hat{\eta}^t$. However, since the essential physics are captured in the component $\hat{\eta}^t_{1212}$, we will only consider this component henceforth and thus write all effective viscosities as scalars. For Newtonian fluids, the effective viscosity in the shear flow will be equal to the viscosity in the straining flow. For suspensions of asymmetric particles, they will differ because the effective viscosity will, in general, depend on the orientations of the particles and the particles follow different trajectories in these flows. It is sufficient to calculate the effective viscosity only in these cases because all linear flows can be written as a linear combination of these two flows.

The flow $(\vec{u},\, p)$ satisfying (1) is a function of the state of the bacteria – their positions and orientations – and, hence, so is $\hat{\eta}^t$:

$$\vec{u} = \vec{u}\left((x^{c,1}, \alpha_1, \beta_1), \ldots (x^{c,n}, \alpha_n, \beta_n)\right), \quad p = p\left((x^{c,1}, \alpha_1, \beta_1), \ldots (x^{c,1}, \alpha_1, \beta_1)\right), \tag{5}$$

$$\hat{\eta}^t = \hat{\eta}_n\left((x^{c,1}, \alpha_1, \beta_1), \ldots (x^{c,n}, \alpha_n, \beta_n)\right). \tag{6}$$

However, the exact states of the bacteria are not known with certainty (due to white noise), so the precise flow $(\vec{u}, p)$ and $\hat{\eta}^t$ are not known either. Furthermore, as the bacteria move, $\hat{\eta}^t$ varies with time. Nevertheless, as a material quantity, $\hat{\eta}$ should be time-independent. The distribution of bacteria evolves from an initial distribution P^0_n to some P^t_n at time t, but the presence of white noise ensures that as $t \to \infty$, P^t_n tends to a unique steady state distribution P^∞_n, which is independent of P^0_n. We then define the effective viscosity of the suspension for a given background flow as the *ensemble averages* with respect P^∞_n:

$$\hat{\eta} = \int \hat{\eta}^t\left((x^{c,1}, \alpha_1, \beta_1), \ldots, (x^{c,n}, \alpha_n, \beta_n)\right) \times P^\infty_n\left((x^{c,1}, \alpha_1, \beta_1), \ldots, (x^{c,n}, \alpha_n, \beta_n)\right) \sin\beta_1\, d\alpha_1\, d\beta_1 \ldots \sin\beta_n\, d\alpha_n\, d\beta_n, \tag{7}$$

where the integral is over the n-fold product of $\mathbb{R}^3 \times S^2$, the space of particle configurations.

2.1. **The dilute limit.** In general, calculating solutions to the full hydrodynamic equations (1) and P^∞_n is a difficult problem, but both become tractable in the dilute limit. Therefore, instead of solving (1), we consider only solutions for a single bacterium in $\mathbb{R}^3$. Specifically, let $\left(\vec{u}^d(\vec{x}, \vec{x}^c, \hat{d}), p^d(\vec{x}, \vec{x}^c, \hat{d})\right)$ denote the flow

due to a single particle with orientation $\hat{d}$ placed in the background flow. It satisfies

$$\left\{ \begin{array}{ll} \eta\Delta\vec{u}^d = \nabla p^d + f_p\hat{d}\delta(\vec{x}-\vec{x}^f) & \vec{x}\in\mathbb{R}^3\setminus B \\ \nabla\cdot\vec{u}^d = 0 & \vec{x}\in\mathbb{R}^3\setminus B \\ \vec{u}^d = \vec{v}+\vec{\omega}\times(\vec{x}-\vec{x}^c) & \vec{x}\in\partial B \\ \vec{u}^d \to E\cdot\vec{x}+\vec{\Omega}\times\vec{x} & \vec{x}\to\infty \end{array} \right\} \tag{8a}$$

along with

$$\left\{ \begin{array}{l} \int_{\partial B}\sigma^d\cdot\nu dx + f_p\hat{d} = 0 \\ \int_{\partial B}\sigma^d\cdot\nu\times(\vec{x}-\vec{x}^c)\,dx + \vec{\tau} = 0 \end{array} \right\}. \tag{8b}$$

The full flow (that is, the dilute approximation to the solution of equation (1)) $\left(\vec{u}^D, p^D\right)$ is then given by

$$\vec{u}^D = E\cdot\vec{x}+\vec{\Omega}\times\vec{x}+\sum_l(\vec{u}^d(\vec{x},\vec{x}^{c,l},\hat{d}^l)-E\cdot\vec{x}-\vec{\Omega}\times\vec{x}) \tag{9a}$$

and

$$p^D = \sum_l p^d(\vec{x},\vec{x}^{c,l},\hat{d}^l). \tag{9b}$$

Additionally, the orientations of the inclusions become independent and P_n^∞ is completely defined by the single particle steady-state distribution P^∞. Thus, here we have

$$P_n^\infty\left((x^{c,1},\alpha_1,\beta_1),\ldots,(x^{c,n},\alpha_n,\beta_n)\right) = \prod_l P^\infty(x^{c,l},\alpha_l,\beta_l). \tag{10}$$

As in previous work on dilute suspensions, we assume that for suspensions with identical particle locations and orientations the following approximation property is true:

$$\hat{\eta}^t(\vec{u}^D,p^D)-\hat{\eta}^t(\vec{u},p) = \mathcal{O}(\phi^2), \tag{11}$$

where $\phi = \frac{4\pi}{3}na^2b$ is the volume fraction and n is the number of bacteria per unit volume.

The single particle distribution $P^\infty(x^c,\alpha,\beta)$ is obtained from (8b) as shown in the next section. Furtheremore, the bulk stress and, therefore, the effective viscosity, become the sum of bulk stresses and effective viscosities of single particle configurations respectively.

$$\hat{\eta}^t\left(\vec{u}^D,p^D\right) = \eta+\hat{\eta}_1(x^{c,1},\alpha_1,\beta_1)+\cdots+\hat{\eta}_1(x^{c,n},\alpha_n,\beta_n), \tag{12}$$

where

$$\hat{\eta}_1(x^c,\alpha,\beta) = \hat{\eta}^t\left(\vec{u}^d(x^c,\alpha,\beta),p^d(x^c,\alpha,\beta)\right). \tag{13}$$

It can be shown that the single particle effective viscosity $\hat{\eta}_1$ is independent of the location of the bacterium x^c and so only the orientational distribution $P^\infty(\alpha,\beta)$ is required to carry out ensemble averaging. Using (10), (12) and (13) in (7) we have, according to (11):

$$\hat{\eta}^t = \eta+n\hat{\eta}_1+\mathcal{O}(\phi^2) = \eta+n\int_{S^2}\hat{\eta}_1(\alpha,\,\beta)P^\infty(\alpha,\,\beta)\,\sin\beta\,d\alpha\,d\beta+\mathcal{O}(\phi^2).$$

We show next how the equations of motion of the orientation vector can be obtained explicitly, which will then lead to the Fokker-Planck equation for P^t.

2.2. **Equations of motion and the Fokker-Planck equation.** For arbitrary given $\vec{v}$ and $\vec{\omega}$, equation (8a) can be viewed as a Dirichlet problem, while the actual values of $\vec{v}$ and $\vec{\omega}$ are determined uniquely through the additional constraints in eq. (8b). The equations of motion follow from solving for $\vec{v}$ and $\vec{\omega}$ from these constraints as follows.

Fix parameters $\vec{r}, \vec{\Omega} \in \mathbb{R}^3$, $a, b, \lambda, D, \eta \in \mathbb{R}^+$ [1], $f_p \in \mathbb{R}$, and $E \in \mathbb{R}^{3\times 3}$, such that E is symmetric and trace-free. Given arbitrary $\vec{x}^c, \vec{v}, \vec{\omega} \in \mathbb{R}^3$ and $\hat{d} \in S^2$ ($\vec{x}^f$ is automatically specified by its definition, $\vec{x}^f := \vec{x}^c + b(1+\lambda)\hat{d}$), there exists a unique solution $(\vec{u}, p)$ (up to an additive constant in the pressure p) to (8a). The existence and uniqueness of this solution is discussed in Appendix B. We write

$$\vec{u} = \vec{U}\left(\vec{x}^c, \hat{d}, \vec{v}, \vec{\omega}\right), \quad p = P\left(\vec{x}^c, \hat{d}, \vec{v}, \vec{\omega}\right),$$

and define functions $\vec{F}$ and $\vec{T}$ (representing the force and torque on the bacterium) from $\mathbb{R}^3 \times S^2 \times \mathbb{R}^3 \times \mathbb{R}^3$ to $\mathbb{R}^3$ as follows:

$$\vec{F}\left(\vec{x}^c, \hat{d}, \vec{v}, \vec{\omega}\right) := \int_{\partial B} \sigma\left(\vec{U}(\vec{x}, \hat{d}, \vec{v}, \vec{\omega}), P(\vec{x}, \hat{d}, \vec{v}, \vec{\omega})\right) \cdot \hat{\nu}\, dx + f_p \hat{d}, \tag{14a}$$

$$\vec{T}\left(\vec{x}^c, \hat{d}, \vec{v}, \vec{\omega}\right) := \int_{\partial B} \sigma\left(\vec{U}(\vec{x}, \hat{d}, \vec{v}, \vec{\omega}), P(\vec{x}, \hat{d}, \vec{v}, \vec{\omega})\right) \cdot \hat{\nu}(x) \times (\vec{x} - \vec{x}^c)\, dx + \vec{\tau}. \tag{14b}$$

For the class of linear background flows $\vec{u}^b = E \cdot \vec{x} + \vec{\Omega} \times \vec{x}$ the functions defined by (14a) and (14b) can be computed explicitly:

$$\begin{aligned} F_i =& -6\pi\eta b v_j \left[X^A d_i d_j + Y^A\left(\delta_{ij} - d_i d_j\right)\right] + f_p d_i \\ =& -6\pi b \eta v N d_i + f_p d_i \end{aligned} \tag{15a}$$

$$\begin{aligned} T_i =& -8\pi\eta b^3 \left[X^C d_i d_j + Y^C\left(\delta_{ij} - d_i d_j\right)\right](\Omega_j - \omega_j) \\ &+ 8\pi\eta b^3 Y^H \epsilon_{ijm} d_m d_k E_{jk} + \tau_i, \end{aligned} \tag{15b}$$

where $v := |\vec{v}|$, ϵ is the Levi-Civita symbol, X^A, Y^A, X^C, Y^C, and Y^H are scalar resistance functions (of the eccentricity e) for the prolate spheroid given in equations (93b-93f) and N is a scalar function of e and λ, given by

$$N := \frac{X^A}{1 - \frac{3X^A}{4e^3}\left[\frac{e(1-e^2)(1+\lambda)}{(1+\lambda)^2 - e^2} - (1+e^2)\operatorname{arctanh}\frac{e}{1+\lambda}\right]}. \tag{16}$$

Plots of N against e are given for various values of λ in Fig. 3.

As can be immediately seen from (15a) and (15b), $\vec{F}$ and $\vec{T}$ are smooth in $(\vec{x}^c, \hat{d}, \vec{v}, \vec{\omega})$ and nondegenerate in the last two variables–that is, $\det\left(\frac{\partial(\vec{F}, \vec{T})}{\partial(\vec{v}, \vec{\omega})}\right) \neq 0$. Imposing the balance of forces and torques yields the system of equations

$$\vec{F}(\vec{x}^c, \hat{d}, \vec{v}, \vec{\omega}) = 0, \quad \vec{T}(\vec{x}^c, \hat{d}, \vec{v}, \vec{\omega}) = 0, \tag{17}$$

which, thanks to the aforementioned nondegeneracy condition, can be solved using the implicit function theorem to yield $(\vec{v}, \vec{\omega})$ as functions of $(\vec{x}^c, \hat{d})$. In the present case (17) is a linear problem in $(\vec{v}, \vec{\omega})$ and solving for these velocities amounts to inverting the resistance matrices H and J defined as

$$H_{ij} := \left[X^A d_i d_j + Y^A\left(\delta_{ij} - d_i d_j\right)\right], \tag{18a}$$

[1] $\mathbb{R}^+ := \{x \in \mathbb{R} : \ x \geq 0\}$.

from equation (15a), and

$$J_{ij} := \left[X^C d_i d_j + Y^C \left(\delta_{ij} - d_i d_j\right)\right], \tag{18b}$$

from equation (15b).

The equations of motion for a single bacterium interacting with a linear background flow are now obtained by demanding that $\vec{v}$, $\vec{\omega}$ define the time derivatives of the position $\vec{x}^c$ and the orientation vector $\hat{d}$ as follows:

$$\frac{d\vec{x}^c}{dt} = \vec{v}\left(\vec{x}^c, \hat{d}\right) = -\frac{f_p}{6\pi b\eta N}\hat{d} \tag{19a}$$

$$\frac{d\hat{d}}{dt} = \vec{\omega}\left(\vec{x}^c, \hat{d}\right) \times \hat{d} = \dot{\hat{d}}^D + \vec{\omega}^R \times \hat{d}, \tag{19b}$$

where $\dot{\hat{d}}^D$ is the effect of the background flow (henceforth referred to as the *drift*) and $\vec{\omega}^R$ is the rotational velocity due to the additional torque $\vec{\tau}$:

$$\dot{d}_i^D = \epsilon_{ijk}\Omega_j d_k + B\left(E_{ij}d_j - d_i E_{jk} d_j d_k\right), \tag{20a}$$

$$\vec{\omega}^R = (8\pi\eta b^3)^{-1} J^{-1} \cdot \vec{\tau}, \tag{20b}$$

where $B := \frac{b^2-a^2}{b^2+a^2}$ is the Bretherton constant.

In order to complete the equations of motion for the orientation vector, we must now specify $\vec{\tau}$ explicitly. It is selected to make $\dot{\hat{d}}^R := \vec{\omega}^R \times \hat{d}$ a white noise process on the unit sphere. This corresponds to

$$\vec{\omega}^R := -\sqrt{2D}\hat{d} \times \begin{pmatrix} -\xi^1 \sin\alpha \sin\beta + \xi^2 \cos\alpha\cos\beta \\ \xi^1 \cos\alpha \sin\beta + \xi^2 \sin\alpha\cos\beta \\ -\xi^2 \sin\beta, \end{pmatrix}. \tag{21}$$

where ξ^i are the derivatives of Wiener processes. $\vec{\tau}$ is then defined by (20b).

The existence and uniqueness of solutions to the system of stochastic differential equations (19) can be established by standard methods. It can be shown that the trajectories of this system exist for all time for any initial condition and are continuous for almost any realization of the noise ξ^i (with respect to the Wiener measure for the rotational Brownian motion; see, e.g., [25, 17, 18]).

In principle, via a standard procedure (namely, the application of Itô's calculus), equations (19a) and (19b) lead directly to a Fokker-Planck equation for $P^t(\vec{x^c}, \hat{d})$, the probability distribution of the position and the orientation of the bacterium at time t. However, the translational dynamics defined by (19a) is irrelevant for our purposes. Indeed, in the dilute limit interparticle interactions are disregarded, while for the interaction with a linear background flow changing the position of the bacterium produces no change in the corresponding bulk stress. This is because, up to translation of the solution, the only difference between solutions of PDE (8) for different values of $\vec{x}^c$ are in the values of $\vec{v}$ ($\vec{v}^1 - \vec{v}^2 = E \cdot \left(\vec{x}^{c,1} - \vec{x}^{c,2}\right)$) and a translating spheroid produces no bulk stress (see, e.g., [21]). Therefore, P^t can be considered as a function of orientation $\hat{d}$ only. Thus, henceforth we fix the location of the spheroid at the origin and consider only the equation of motion for the orientation (19b) with the corresponding deterministic drift $\dot{\hat{d}}^D$ and noise $\vec{\omega}^R$.

Below we will consider various background flows corresponding to different strain rate matrices E and vorticity vectors $\vec{\Omega}$, which will in each case define $\dot{\hat{d}}^D$. The random part $\vec{\omega}^R$, however, is fixed, so we can write the general Fokker-Planck

equation for $P^t(\hat{d}) = P(\alpha, \beta, t)$, the probability distribution of orientations $\hat{d}$ at time t written in terms of the azimuthal and the polar angles on the sphere (α, β):

$$\frac{\partial P}{\partial t} = -\nabla_{\alpha,\beta} \cdot \left(P \dot{\hat{d}}^D \right) + D \Delta_{\alpha,\beta} P, \tag{22}$$

where D is a constant specifying the strength of rotational diffusion, $\Delta_{\alpha,\beta}$ is the spherical laplacian, given by

$$\Delta_{\alpha,\beta} = \frac{1}{\sin^2\beta} \frac{\partial^2}{\partial \alpha^2} + \frac{\cos\beta}{\sin\beta} \frac{\partial}{\partial \beta} + \frac{\partial^2}{\partial \beta^2}, \tag{23}$$

and $\nabla_{\alpha,\beta}$ is the spherical gradient, given by

$$\nabla_{\alpha,\beta} = \begin{pmatrix} -\frac{\sin\alpha}{\sin\beta} \frac{\partial}{\partial \alpha} + \cos\alpha\cos\beta \frac{\partial}{\partial \beta} \\ \frac{\cos\alpha}{\sin\beta} \frac{\partial}{\partial \alpha} + \sin\alpha\cos\beta \frac{\partial}{\partial \beta} \\ -\sin\beta \frac{\partial}{\partial \beta} \end{pmatrix}. \tag{24}$$

As mentioned at the beginning of this section, we are interested in ensemble averages with respect to the steady state distribution of $\hat{d}$, that is, with respect to the solution P^∞ of the time-independent Fokker-Planck equation obtained from 22 by setting $\frac{\partial P^\infty}{\partial t} = 0$:

$$\nabla_{\alpha,\beta} \cdot \left(P^\infty \dot{\hat{d}}^D \right) = D \Delta_{\alpha,\beta} P^\infty. \tag{25}$$

The convergence of $P \to P^\infty$ as $t \to \infty$ in $L^1(S^2)$ is shown in [28].

3. **The bulk stress.** The bulk deviatoric stress of the system with a single spheroid depends only on the instantaneous configuration of the spheroid with respect to the background flow. Thus, we calculate this bulk deviatoric stress here in general, for an arbitrary linear background flow characterized by the strain rate matrix E and the vorticity vector $\vec{\Omega}$. As explained in the previous section, this stress is independent of the location of the spheroid $\vec{x}^c$ and is only a function of its orientation. Since a particle's orientation is unknown, we then average over orientations.

The bulk deviatoric stress due to one inclusion is defined by

$$\Sigma^l_{ij} := \frac{1}{|V|} \int_{S^2} \int_V \left(\sigma_{ij}(\alpha^l, \beta^l) - \frac{1}{3} \delta_{ij} \sigma_{kk}(\alpha^l, \beta^l) \right) P^\infty(\alpha^l, \beta^l) dx dS, \tag{26}$$

where V is any volume containing the entire suspension (the value of the integral is independent of this choice). Here, we average over orientations because α and β are random variables. For a dilute suspension, we define the bulk deviatoric stress of the entire suspension to be

$$\Sigma_{ij} := \sum_l \Sigma^l_{ij}. \tag{27}$$

Since (α^l, β^l) are independent identically distributed random variables, $\Sigma^m = \Sigma^n$ $\forall m, n$, so we can rewrite this as

$$\Sigma_{ij} = n \Sigma^l_{ij}, \tag{28}$$

for any fixed l.

We summarize our results on the bulk deviatoric stress in

Proposition 1. *The bulk deviatoric stress in a bacterial suspension modeled by PDE (1) is given by*

$$\begin{aligned}\Sigma_{ij} =& 2\eta E_{ij} + \frac{5b^2}{a^2}\phi\eta \int_{S^2} \Lambda_{ijkl} P^\infty dS E_{kl} \\ &- 3\eta\phi B Y^H \frac{b^2}{a^2} \int_{S^2} (\epsilon_{ikl} d_j + \epsilon_{jkl} d_i) d_l \epsilon_{kmn} d_m d_n P^\infty dS E_{mn} \\ &+ 3\eta\phi Y^H \frac{b^2}{a^2} D \int_{S^2} (\epsilon_{ikl} d_j + \epsilon_{jkl} d_i) d_l \epsilon_{kmn} d_m (\partial_n P^\infty) dS \\ &+ \frac{f_p}{16\pi a^2}\phi K \int_{S^2} (\delta_{ij} - 3 d_i d_j) P^\infty dS + \mathcal{O}(\phi^2),\end{aligned} \tag{29}$$

where ϕ is the volume fraction, Λ is a function of shape and orientation given in equation (34), Y^H is a scalar function of eccentricity e given in equation (93f), and K is a scalar function of e and λ given in (42) and plotted in Fig. 4.

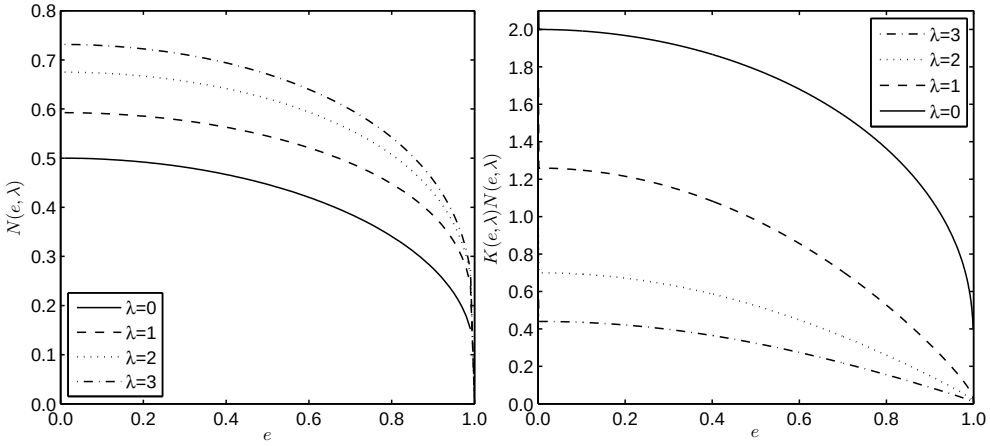

FIGURE 3. N vs. e and KN vs. e for various values of λ

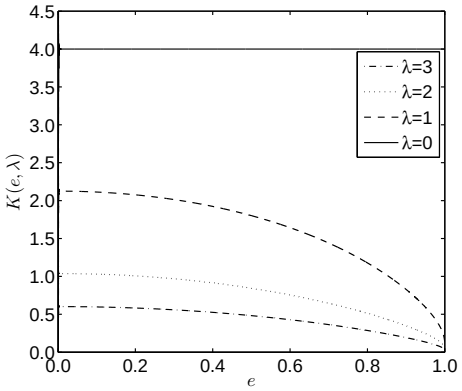

FIGURE 4. K vs. e for various values of λ

We calculate Σ by splitting it into passive, tumbling, and active contributions. We write $\vec{u}^d = \vec{u}^p + \vec{u}^t + \vec{u}^a$, where

$$\begin{cases} \eta\Delta\vec{u}^p = \nabla p^p & x \in \mathbb{R}^3 \setminus B \\ \nabla\cdot\vec{u}^p = 0 & \vec{x} \in \mathbb{R}^3 \setminus B \\ \vec{u}^p = \vec{\omega}^p \times (\vec{x} - \vec{x}^c) + \vec{v}^p & \vec{x} \in \partial B \\ \vec{u}^p \to E\cdot\vec{x} + \vec{\Omega}\times\vec{x} & \vec{x} \to \infty \\ \int_{\partial B} \sigma^p\cdot\hat{\nu}\times(\vec{x}-\vec{x}^c)dx = 0 & \\ \int_{\partial B} \sigma^p\cdot\hat{\nu}dx = 0 & \end{cases} \tag{30}$$

describes interaction of a passive spheroid with the background flow,

$$\begin{cases} \eta\Delta\vec{u}^t = \nabla p^t & x \in \mathbb{R}^3 \setminus B \\ \nabla\cdot\vec{u}^t = 0 & \vec{x} \in \mathbb{R}^3 \setminus B \\ \vec{u}^t = \vec{\omega}^t \times (\vec{x} - \vec{x}^c) & \vec{x} \in \partial B \\ \vec{u}^t \to 0 & \vec{x} \to \infty \\ \int_{\partial B} \sigma^t\cdot\hat{\nu}\times(\vec{x}-\vec{x}^c)dx + \vec{\tau}\ ^2 = 0 & \end{cases} \tag{31}$$

describes the effects of tumbling, and

$$\begin{cases} \eta\Delta\vec{u}^a = \nabla p^a + f_p\hat{d}\delta(\vec{x} - \vec{x}^f) & x \in \mathbb{R}^3 \setminus B \\ \nabla\cdot\vec{u}^a = 0 & \vec{x} \in \mathbb{R}^3 \setminus B \\ \vec{u}^a = \vec{v}^a & \vec{x} \in \partial B \\ \vec{u}^a \to 0 & \vec{x} \to \infty \\ \int_{\partial B} \sigma^a\cdot\hat{\nu}dx + f_p\hat{d} = 0 & \end{cases} \tag{32}$$

describes the effects of forward self-propulsion. We then define Σ^p, Σ^t and Σ^a as the bulk stress in problem (30), (31) and (32), respectively.

Σ^p is calculated in [21] and is given by

$$\begin{aligned} \Sigma^p_{ij} =& 2\eta E_{ij} + \frac{5b^2}{a^2}\phi\eta\int_{S^2}\Lambda_{ijkl}P^\infty dS E_{kl} \\ &- 3\eta\phi B Y^H\frac{b^2}{a^2}\int_{S^2}(\epsilon_{ikl}d_j + \epsilon_{jkl}d_i)d_l\epsilon_{kmn}d_m d_n P^\infty dS E_{mn}, \end{aligned} \tag{33}$$

where ϕ is the volume fraction of the suspension, Y^H is a scalar function of e given in equation (93f), and

$$\Lambda_{ijkl} = X^M d^0_{ijkl} + Y^M d^1_{ijkl} + Z^M d^2_{ijkl}, \tag{34}$$

where

$$\begin{aligned} d^0_{ijkl} =& \frac{3}{2}\left(d_i d_j - \frac{1}{3}\delta_{ij}\right)\left(d_k d_l - \frac{1}{3}\delta_{kl}\right) \\ d^1_{ijkl} =& \frac{1}{2}\left(d_i\delta_{jl}d_k + d_j\delta_{il}d_k + d_i\delta_{jk}d_l + d_j\delta ikd_l - 4d_i d_j d_k d_l\right) \\ d^2_{ijkl} =& \frac{1}{2}\left(\delta_{ik}\delta_{jl} + \delta_{jk}\delta_{il} - \delta_{ij}\delta_{kl} + d_i d_j\delta_{kl} + \delta_{ij}d_k d_l\right. \\ & \left. -d_i\delta_{jl}d_k - d_j\delta_{il}d_k - d_i\delta_{jk}d_l - d_j\delta_{ik}d_l + d_i d_j d_k d_l\right), \end{aligned} \tag{35}$$

and X^M, Y^M, and Z^M are scalar functions of e given in equations (93g), (93h), and (93i), respectively. The first term on the right hand side of eq. (33) is the

[2] It is shown in [6] that, when performing the averaging over orientations in eq. (26), $\vec{\tau}$, a white noise process, can be replaced by $\vec{\tau}^\infty$ where $\vec{\tau}^\infty = 8\pi\eta b^3 J\vec{\omega}^{R,\infty}$, with J defined in eq. (18), and $\vec{\omega}^{R,\infty} := -D\hat{d}\times\nabla_{\alpha,\beta}\log(P^\infty)$.

standard Newtonian deviatoric stress. The second and third terms represent the passive contributions due to the presence of spheroids.

Σ^t is calculated in [15] [3] and is given by

$$\Sigma^t_{ij} = 3\eta\phi Y^H \frac{b^2}{a^2} D \int_{S^2} (\epsilon_{ikl} d_j + \epsilon_{jkl} d_i) d_l \epsilon_{kmn} d_m (\partial_n P^\infty) dS. \tag{36}$$

It remains to calculate Σ^a. We do this by further decomposing $\vec{u}^a$ by writing $\vec{u}^a = \vec{u}^{a,1} + \vec{u}^{a,2} + \vec{u}^{a,3}$, where

$$\begin{cases} \eta\Delta\vec{u}^{a,1} = \nabla p^{a,1} + f_p \hat{d}\delta(\vec{x} - \vec{x}^f) & \vec{x} \in \mathbb{R}^3 \\ \nabla \cdot \vec{u}^{a,1} = 0 & \vec{x} \in \mathbb{R}^3 \\ \vec{u}^{a,1} \to 0 & \vec{x} \to \infty, \end{cases} \tag{37}$$

$$\begin{cases} \eta\Delta\vec{u}^{a,2} = \nabla p^{a,2} & \vec{x} \in \mathbb{R}^3 \setminus B \\ \nabla \cdot \vec{u}^{a,2} = 0 & x \in \mathbb{R}^3 \setminus B \\ \vec{u}^{a,2} = -\vec{u}^{a,1} & x \in \partial B \\ \vec{u}^{a,2} \to 0 & \vec{x} \to \infty \end{cases} \tag{38}$$

and

$$\begin{cases} \eta\Delta\vec{u}^{a,3} = \nabla p^{a,3} & \vec{x} \in \mathbb{R}^3 \setminus B \\ \nabla \cdot \vec{u}^{a,3} = 0 & \vec{x} \in \mathbb{R}^3 \setminus B \\ \vec{u}^{a,3} = \vec{v}^a & \vec{x} \in \partial B \\ \vec{u}^{a,3} \to 0 & \vec{x} \to \infty \\ \int_{\partial B} \left(\sigma^{a,1} + \sigma^{a,2} + \sigma^{a,3}\right) \cdot \hat{\nu} dx + f_p \hat{d} = 0. \end{cases} \tag{39}$$

$\vec{u}^{a,3}$ is the flow due to a translating spheroid and $\vec{u}^{a,1}$ is a force monopole, both of which produce no bulk stress. The bulk stress due to $\vec{u}^{a,2}$ can be calculated without actually solving the problem by applying Faxén's law for prolate spheroids (see [21]):

$$\begin{aligned} \Sigma^{a,2}_{ij}(\hat{d}) = &-\frac{5}{2e^3}\pi\eta\Lambda_{ijkl} \\ &\times \int_{-be}^{be} \left((be)^2 - \upsilon^2\right) \left[1 + ((be)^2 - \upsilon^2)\frac{1-e^2}{8e^2}\Delta\right] \left(\frac{\partial u^{a,1}_k}{\partial x_l} + \frac{\partial u^{a,1}_l}{\partial x_k}\right)\Bigg|_{\hat{d}\upsilon} d\upsilon. \end{aligned} \tag{40}$$

Performing the integration in equation (40) and averaging over orientations, we get

$$\Sigma^a_{ij} = \Sigma^{a,2}_{ij} = \frac{f_p}{16\pi a^2}\phi K \int_{S^2} (\delta_{ij} - 3d_i d_j) P^\infty dS, \tag{41}$$

where

$$\begin{aligned} K = 15X^M \Bigg[&\frac{3(1+\lambda)^2 - e^2(3+\lambda(2+\lambda))}{e^4(e^2-(1+\lambda)^2)} \\ &-\frac{1}{e^5}\left(3-e^2\right)(1+\lambda)\,\mathrm{arctanh}\frac{e}{(1+\lambda)}\Bigg] \end{aligned} \tag{42}$$

and X^M is given in equation (93g). A plot of K against e is given for various values of λ in Fig. 4.

Combining equations (33), (36), and (41), we get equation (29).

[3] The stress due to tumbling in our model is equivalent to the diffusive stress due to the Brownian motion of fluid particles calculated in [15]. This is because both effects produce bulk hydrodynamic stress through the random rotation of the particle $\vec{\omega}^R$, which is equal in both cases.

4. **The effective viscosity.** In order to calculate the effective viscosity, it remains to select a background flow and calculate the corresponding solution P^∞ to eq. (25). Choosing a planar background flow allows one to define an effective viscosity through the ratio of one component of the bulk deviatoric stress Σ to the rate of strain γ (e.g., for flows in the x, y plane, we can define $\hat{\eta} := \frac{\Sigma_{12}}{\gamma}$). Without loss of generality, we study two general flows (for a discussion of why these are sufficient, see section 2): a planar shear flow in the x, y plane, described by

$$E = \frac{1}{2}\begin{pmatrix} 0 & \gamma & 0 \\ \gamma & 0 & 0 \\ 0 & 0 & 0 \end{pmatrix} \tag{43a}$$

with

$$\vec{\Omega} = \left(0, 0, \frac{\gamma}{2}\right) \tag{43b}$$

and a planar straining flow in the x, y plane, described by

$$E = \frac{1}{2}\begin{pmatrix} 0 & \gamma & 0 \\ \gamma & 0 & 0 \\ 0 & 0 & 0 \end{pmatrix} \tag{44a}$$

with

$$\vec{\Omega} = (0, 0, 0)\,. \tag{44b}$$

For dilute suspensions of rotationally symmetric particles, there is no difference to the viscosity in these cases. This is because the addition of vorticity in the case of the planar shear flow simply causes the particle to rotate rigidly with the background flow with a rotational velocity $\vec{\omega}^D$ equal to the vorticity $\vec{\Omega}$. The rotational contribution to the bulk stress is proportional to $\vec{\Omega} - \vec{\omega}^D$ (see, e.g., [21]), but this is zero. Additionally, rotational asymmetry means that P^∞ will be different for the two flows, whereas for rotationally symmetric particles $P^\infty = \frac{1}{4\pi}$ for all flows because there can be no preferred orientation.

Neither of the above background flows produces a Fokker-Planck equation that can be solved analytically. Therefore, we solve them asymptotically in various parameters and numerically in the general case.

For the flow without vorticity (eqs. (44a), (44b)), our results are summarized in

Proposition 2. *The effective viscosity in a bacterial suspension modeled by PDE (1) in a planar straining flow (e.g., eq. (44a)) is given asymptotically by*

$$\hat{\eta} = \eta + \eta\phi\left[S - \frac{f_p}{16\pi a^2 \gamma\eta} K + \mathcal{O}\left(\frac{1}{\mu}\right)\right] + \mathcal{O}(\phi^2), \quad f_p = 6\pi b\eta v N \tag{45}$$

when $\mu := \frac{\gamma B}{D} \gg 1$ (i.e., the background flow dominates rotational diffusion due to tumbling and the bacteria are non-spherical) and by

$$\hat{\eta} = \eta + \eta\phi\left[M_0 - \frac{f_p K}{160\pi a^2 \gamma\eta}\mu + M_2\mu^2 + \mathcal{O}\left(\mu^3\right)\right] + \mathcal{O}(\phi^2), \quad f_p = 6\pi b\eta v N \tag{46}$$

when $\mu \ll 1$ (i.e., the bacteria have a weak tendency to align either because of being nearly spherical or because the background flow is dominated by diffusion). In the above equations, K and N are scalar functions of e and λ, given in equations (42) and (16), respectively, and S, M_0, and M_2 are scalar functions of e given in equations (53), (74a), and (74b), respectively. S, M_0, and M_2 are plotted in Fig. 7, K is plotted in Fig. 4, and and N and NK are plotted in Fig. 3.

Formulas (45) and (46), as well as corresponding numerics, are plotted in Fig. 5, using values established in the literature for *B. Subtilis*. It is assumed that the bacteria have dimensions $b = 4\mu$m, $\frac{b}{a} = 5.7$ (see [32]), and $\lambda = 0.5$. We assume a bacterial swimming speed $v = 50\mu\text{m s}^{-1}$ (observed when swimming collectively; this determines f_p via eq. (15a)) and a rotational diffusion constant $D = 0.017\text{s}^{-1}$ (see [31]).

Both formulas (45) and (46) predict a decrease in viscosity due to self-propulsion, which is represented by the third term in both equations. While equation (45) is not valid for $B = 0$ (spheres), equation (46) demonstrates the importance of asymmetry due to the fact that the active term vanishes when $B \to 0$. Note that η shows up in the denominator in the active terms because f_p is proportional to η (see eq. (15a)). The passive terms in both formulas agree with those derived in [15]. A striking feature of formula (46) is the fact that the active contributions do not disappear in the limit $\gamma \to 0$ (note that eq. (45) is not valid in this limit). This is counterintuitive because as $\gamma \to 0$, $P^\infty \to \frac{1}{4\pi}$ and hence the active contribution to the bulk deviatoric stress Σ^a averages to zero. However, for small γ, $P^\infty = \frac{1}{4\pi} + C\gamma + \mathcal{O}\left((\gamma)^2\right)$ and Σ^a acquires a contribution proportional to γ. When calculating Σ^a from P^∞, the constant term (in γ) averages to zero, but the linear term remains. Hence, the active contribution to the effective viscosity $\hat{\eta}^a := \frac{\Sigma^a}{\gamma}$ contains a non-vanishing term. However, in reality, the time it takes for a suspension to reach the steady state P^∞ increases as $\gamma \to 0$. Thus, for small enough γ, rotatinal diffusion due to tumbling will dominate advection and the actual P^∞ will be closer to $\frac{1}{4\pi}$, which produces $\hat{\eta}^a = 0$.

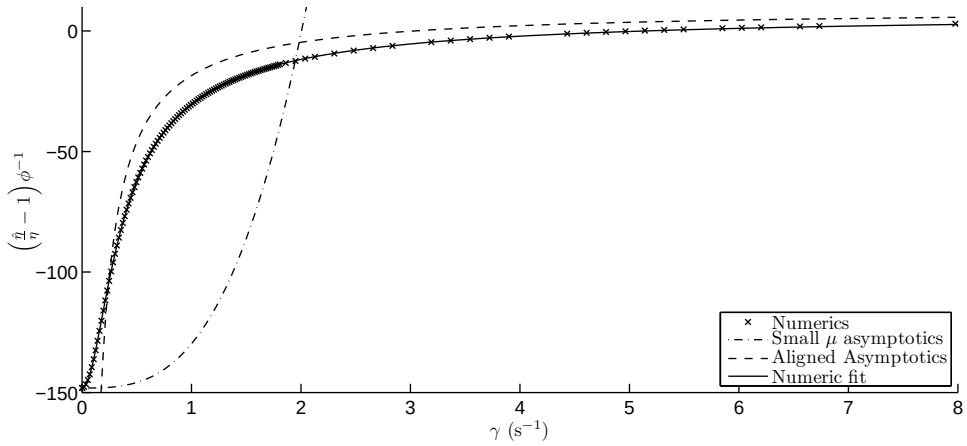

FIGURE 5. $\left(\frac{\hat{\eta}}{\eta} - 1\right)\phi^{-1}$ vs. γ for the case of no vorticity ($\vec{\Omega} = (0,0,0)$) evaluated numerically along with small μ asymptotics (eq. (46)) and large $\frac{\gamma}{D}$ asymptotics (eq. (45)).

For the flow with vorticity (eqs. (43a), (43b)), our results are summarized in

Proposition 3. *The effective viscosity in a bacterial suspension modeled by PDE (1) in a planar shear flow (e.g., eq. (43a)) is given asymptotically by*

$$\hat{\eta} = \eta + \eta\phi\left[\frac{5}{2} - \frac{9f_pD(5\lambda^2+10\lambda+2)}{20a^2\pi\eta(36D^2+\gamma^2)(1+\lambda)^4}\epsilon + \mathcal{O}(\epsilon^2)\right] + \mathcal{O}(\phi^2), \quad f_p = 6\pi b\eta v N \tag{47}$$

when $\epsilon := \frac{b}{a} - 1 \ll 1$ *(i.e., the bacteria are nearly spherical) and by*

$$\hat{\eta} = \eta + \eta\phi\left[M_0 - K\frac{9Bf_pD}{40\pi a^2\eta(36D^2+(\omega^0)^2)} + \mathcal{O}\left(\frac{\gamma}{D}\right)\right] + \mathcal{O}(\phi^2), \quad f_p = 6\pi b\eta v N \tag{48}$$

when the shear flow oscillates with frequency ω^0 *and* $\frac{\gamma}{D} \ll 1$ *(i.e., the background flow is very weak compared to rotational diffusion due to tumbling).*

Formulas (47) and (48), as well as numerics, are plotted in Fig. 6, using values established in the literature for *B. Subtilis*.

Once again, formulas (47) and (48) demonstrate a decrease in the effective viscosity due to self-propulsion, the effect of which is captured in the third term of both formulas. While equation (48) is valid only for $\frac{\gamma}{D} \ll 1$, equation (47) demonstrates a curious result: the active contribution to the effective viscosity vanishes as $\frac{D}{\gamma} \to 0$. Apparently, tumbling is *necessary* in order to achieve a reduction in the effective viscosity in shear flows in the absense of interactions between bacteria. This can be explained by the probability density function P^∞ used (see section 4.2 below) in order to derive equation (47) (taken from [15]):

$$P^\infty = \frac{1}{4\pi}\left[1 + B\frac{3\sin^2\beta\sin\left(2\alpha - \arctan\frac{\gamma}{6D}\right)}{2\sqrt{1+\left(\frac{6D}{\gamma}\right)^2}}\right] + \mathcal{O}(B^2). \tag{49}$$

When $\frac{D}{\gamma} = 0$, this distribution is symmetric in α about $\alpha = \frac{\pi}{2}$. When plugged into the active term of the bulk stress (eq. (41)), which has the angular dependence $-\sin 2\alpha \sin^2\beta$, the term vanishes due to integration in α. When $\frac{D}{\gamma} \to \infty$, however, the distribution is symmetric in α about $\alpha = \frac{\pi}{4}$, producing a negative active contribution. As before, the passive terms in both formulas agree with those in [15]. For a discussion of the limit $\gamma \to 0$, see the paragraphs following Proposition 2.

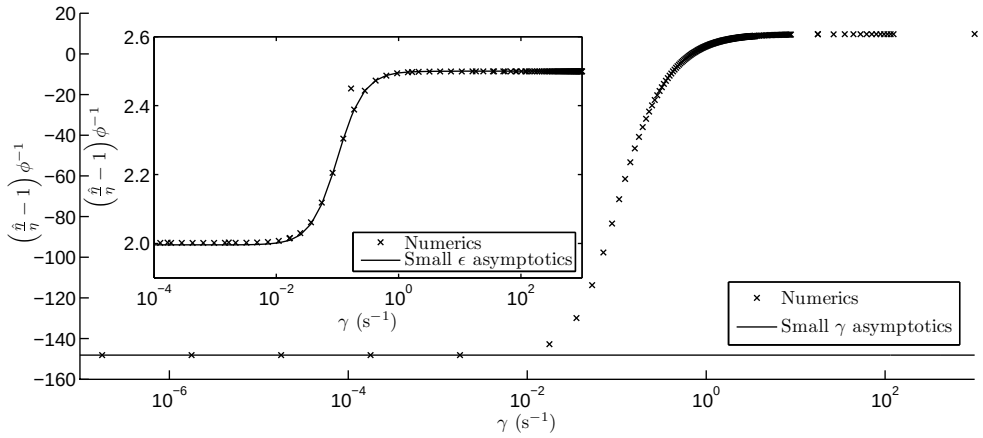

FIGURE 6. $\left(\frac{\hat{\eta}}{\eta} - 1\right)\phi^{-1}$ vs. γ for the case with vorticity evaluated numerically along with small $\frac{\gamma}{D}$ asymptotics (eq. (48)). The inset contains $\left(\frac{\hat{\eta}}{\eta} - 1\right)\phi^{-1}$ vs. γ for the case with small ϵ evaluated numerically along with small ϵ asymptotics (eq. (47)).

The derivation and discussion of these formulas along with an explanation of the numerics are in the following section. In section 4.1, we study bacteria in a purely straining flow in the case when $\mu := \frac{\gamma B}{D} \to \infty$ (i.e., when bacteria have a strong tendency to align with the dynamically stable principal axis of the flow) and obtain eq. (45). This facilitates comparison with our previous results in [11], where tumbling was not included in the model. In section 4.2, we calculate the effective viscosity for a pure shear flow, which is the flow that has been used for much previous analysis (in, e.g., [15]), to produce eq. (47). In section 4.3, we calculate the effective viscosity for a flow without vorticity, as this flow has a steady state axis along which bacteria will align, to produce eq. (45). Since bacteria tend to align when observed in nature, it is expected that this flow would best represent bacteria in nature. In section 4.4 we calculate the effective viscosity for an oscillatory shear flow, since this is the type of flow typically used to measure viscosity in experiments, to produce eq. (48). Finally, in section 4.5, we present numerics done for flows with and without vorticity in order to establish regions of validity for the asymptotic results and to determine the behavior of the effective viscosity between these regions. The numerics are plotted along with the relevant asymptotic formulae in Figures 5 and 6 above.

4.1. **In full alignment with the background flow ($\frac{\gamma B}{D} \to \infty$).** We consider the purely straining background flow described by

$$E = \frac{1}{2}\begin{pmatrix} 0 & \gamma & 0 \\ \gamma & 0 & 0 \\ 0 & 0 & 0 \end{pmatrix} \tag{50}$$

$$\vec{\Omega} = (0,0,0)\,. \tag{51}$$

In the limit $\mu := \frac{\gamma B}{D} \to \infty$, all bacteria will tend to align in the orientations $(\alpha,\beta) = \left(\frac{\pi}{4}, \frac{\pi}{2}\right)$ or $(\alpha,\beta) = \left(\frac{5\pi}{4}, \frac{\pi}{2}\right)$. Therefore, we have

$$P^{\infty} = \left[C\delta\left(\alpha - \frac{\pi}{4}\right) + (1-C)\delta\left(\alpha - \frac{5\pi}{4}\right)\right]\delta\left(\beta - \frac{\pi}{2}\right) + \mathcal{O}\left(\frac{1}{\mu}\right),$$

with $0 \le C \le 1$, yielding an effective viscosity of

$$\hat{\eta} := \frac{\Sigma_{12}}{\dot{\gamma}} = \eta + \left[S\eta - \frac{f_p}{16\pi a^2 \dot{\gamma}} K + \mathcal{O}\left(\frac{1}{\mu}\right)\right]\phi + \mathcal{O}(\phi^2) \tag{52}$$

where K is a scalar function of e and λ, given in equation (42) and plotted in Fig. 4, and S is a scalar function of e, given by

$$S = \frac{5b^2}{8a^2}\left(3X^M + Z^M\right), \tag{53}$$

where X^M and Z^M are scalar resistance functions given in equations (93g) and (93h), respectively. A plot of S against e is given in Fig. 7. The second term in equation (52) represents the passive contribution and the third the active contribution. Since $K > 0$, there is, as before, a decrease in effective viscosity due to self-propulsion. Note that this formula is not valid for $B = 0$ (spherical bacteria), since this is incompatible with the assumption that $\frac{\gamma B}{D} \to \infty$. Using equation (15a), one can write equation (52) in terms of v (for $f_p > 0$).

The normal stress differences are given by

$$\frac{\Sigma_{11}-\Sigma_{22}}{\gamma^2}=0 \tag{54}$$

$$\frac{\Sigma_{22}-\Sigma_{33}}{\gamma^2}=\left[\eta\frac{15b^2(X^M-Z^M)}{8a^2\gamma}-\frac{3f_pK}{32a^2\pi\gamma^2}+\mathcal{O}\left(\frac{1}{\mu}\right)\right]\phi+\mathcal{O}(\phi^2). \tag{55}$$

The results here contrast with those in [29] in that the first normal stress difference is zero. Nevertheless, as in [29], the active contribution to the second normal stress difference is negative for "pushers" ($f_p>0$, the case for most bacteria) and positive for "pullers" ($f_p<0$, the case for some motile unicellular algae).

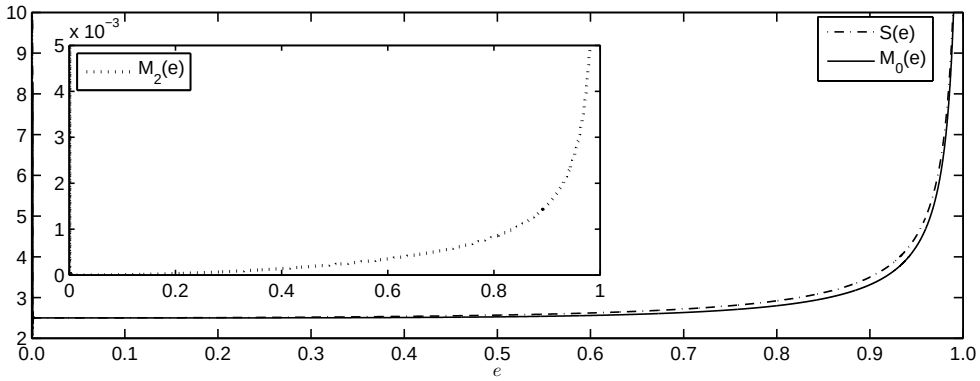

FIGURE 7. M_0, M_2, and S vs. e

4.2. **Nearly spherical bacteria in a background flow with vorticity.** We next consider the case of effective viscosity for near-spheres because the Fokker-Planck equation can be solved asymptotically in this regime.

In the case of

$$E=\frac{1}{2}\begin{pmatrix}0&\gamma&0\\ \gamma&0&0\\ 0&0&0\end{pmatrix} \tag{56}$$

$$\vec{\Omega}=\left(0,0,\frac{\gamma}{2}\right), \tag{57}$$

the deterministic part of the spheroids' orbits, obtained from equation (20a), is described by

$$\begin{cases}\dot{\alpha}^D=\frac{\gamma}{2}\left(1+B\cos 2\alpha\right)\\ \dot{\beta}^D=\frac{B\gamma}{4}\sin 2\alpha\sin 2\beta.\end{cases} \tag{58}$$

Plugging this into equation (25) yields the Fokker-Planck equation

$$\begin{aligned}0=&\frac{B\gamma}{2}\sin 2\alpha\sin\beta\left(3P^\infty\sin\beta-\frac{\partial P^\infty}{\partial\beta}\cos\beta\right)\\ &-\frac{\gamma}{2}\left(1+B\cos 2\alpha\right)\frac{\partial P^\infty}{\partial\alpha}+D\Delta_{\alpha,\beta}P^\infty,\end{aligned} \tag{59}$$

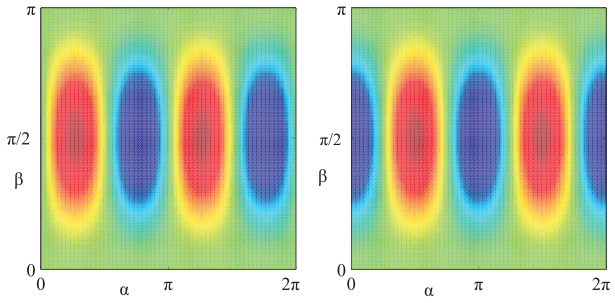

FIGURE 8. Plot of P^∞ for $B \ll 1$, given by equation (60) for (a) $\frac{\gamma}{6D} = 0.1$ and (b) $\frac{\gamma}{6D} = 100$. Darker regions indicate the peaks and troughs. On the left (a), the peaks (red) are located at approximately $\alpha = \frac{\pi}{4}, \frac{5\pi}{4}$ with $\beta = \frac{\pi}{2}$. On the right (b), the peaks (red) are located at approximately $\alpha = \frac{\pi}{2}, \frac{3\pi}{2}$ with $\beta = \frac{\pi}{2}$.

where $\Delta_{\alpha,\beta}$ is the spherical laplacian, given in equation (23). We can then take P^∞, asymptotic in $B := \frac{(1+\epsilon)^2-1}{(1+\epsilon)^2+1}$, where $\epsilon := \frac{b}{a} - 1$, from [15]–

$$P^\infty = \frac{1}{4\pi}\left[1 + B\frac{3\sin^2\beta\sin\left(2\alpha - \arctan\frac{\gamma}{6D}\right)}{2\sqrt{1+\left(\frac{6D}{\gamma}\right)^2}}\right] + \mathcal{O}(B^2). \tag{60}$$

A plot of P^∞ is given for two different values of $\frac{\gamma}{D}$ in Figure 8.

Using equation (29), we get the asymptotic effective viscosity

$$\begin{aligned}\hat{\eta} = \frac{\Sigma_{12}}{\dot{\gamma}} =& \eta + \phi\left[\frac{5}{2}\eta\right. \\ &\left. - \frac{9f_pD(5\lambda^2+10\lambda+2)}{20a^2\pi(36D^2+\gamma^2)(1+\lambda)^4}\epsilon + \mathcal{O}(\epsilon^2)\right] + \mathcal{O}(\phi^2).\end{aligned} \tag{61}$$

Here, the first term is the viscosity of the ambient fluid, the second term is the passive contribution due to a suspension of spheres, and the third term is the contribution due to self-propulsion. As in [15], the passive effect differs from that of a sphere at $\mathcal{O}(\epsilon^2)$. Assuming $f_p > 0$, one can use equation (15a) to rewrite equation (61) in terms of v.

The normal stress differences are given by

$$\frac{\Sigma_{11} - \Sigma_{22}}{\dot{\gamma}^2} = \left[\frac{3f_p(5\lambda^2+10\lambda+2)}{20\pi a^2(36D^2+\gamma^2)(1+\lambda)^4}\epsilon + \mathcal{O}(\epsilon^2)\right]\phi + \mathcal{O}(\phi^2) \tag{62}$$

$$\frac{\Sigma_{22} - \Sigma_{33}}{\dot{\gamma}^2} = \left[-\frac{3f_p(5\lambda^2+10\lambda+2)}{40\pi a^2(36D^2+\gamma^2)(1+\lambda)^4}\epsilon + \mathcal{O}(\epsilon^2)\right]\phi + \mathcal{O}(\phi^2). \tag{63}$$

Once again, the active contribution is $\mathcal{O}(\epsilon)$ while the passive contribution is $\mathcal{O}(\epsilon^2)$. The signs of the active contribution also match the results in [29]–namely, active contribution to the first stress difference is positive for "pushers" ($f_p > 0$) and negative for "pullers" ($f_p < 0$), and vice versa for the second stress difference.

4.3. **Background flow without vorticity, $\frac{\gamma B}{D} \ll 1$.** We now consider the case of $\mu := \frac{\gamma B}{D} \ll 1$ (i.e., bacteria have a weak tendency to align with the background flow

due to being nearly-spherical or weak advection), once more because the Fokker-Planck equation can be solved asymptotically in this regime.

In the case of

$$E = \frac{1}{2}\begin{pmatrix} 0 & \gamma & 0 \\ \gamma & 0 & 0 \\ 0 & 0 & 0 \end{pmatrix} \tag{64}$$

$$\vec{\Omega} = (0,0,0)\,, \tag{65}$$

the deterministic part of the particle trajectories is described by

$$\begin{cases} \dot{\alpha}^D = \frac{B\gamma}{2}\cos 2\alpha \\ \dot{\beta}^D = \frac{B\gamma}{4}\sin 2\alpha \sin 2\beta. \end{cases} \tag{66}$$

Constructing $\dot{\hat{d}}^D$ from this and plugging these into equation (25) leads to the steady state Fokker-Planck equation

$$\begin{aligned} 0 =& \frac{\mu}{2}\sin 2\alpha \sin\beta \left(3P^\infty \sin\beta - \frac{\partial P^\infty}{\partial \beta}\cos\beta\right) \\ & - \frac{\mu}{2}\cos 2\alpha \frac{\partial P^\infty}{\partial \alpha} + \Delta_{\alpha,\beta} P^\infty, \end{aligned} \tag{67}$$

where $\Delta_{\alpha,\beta}$ is the spherical laplacian, given in equation (23). Writing $P^\infty(\alpha,\beta) = \sum_{n=0}^\infty P_n^\infty(\alpha,\beta)\mu^n$, we get

$$\begin{cases} \Delta_{\alpha,\beta} P_0^\infty = & 0 \\ \Delta_{\alpha,\beta} P_{n+1}^\infty = & -\cos\alpha \sin\alpha \sin\beta \left(3\sin\beta P_n^\infty - \cos\beta \frac{\partial P_n^\infty}{\partial \beta}\right) \\ & + \frac{1}{2}\cos 2\alpha \frac{\partial P_n^\infty}{\partial \alpha} \qquad\qquad n \geq 0. \end{cases} \tag{68}$$

The term P_0^∞ corresponds to $B = 0$ or $\gamma = 0$, both of which lead to no alignment, so $P_0^\infty = \frac{1}{4\pi}$ and hence $\Delta_{\alpha,\beta} P_1^\infty = -\frac{3}{8\pi}\sin 2\alpha \sin^2\beta$, which has the two dimensional family of solutions

$$\begin{aligned} P_1^\infty = \frac{1}{64\pi}\frac{\sin 2\alpha}{\sin^2\beta}\big[&(C_1 + 6\cos 2\beta)\left(1+\cos^2\beta\right) \\ &+2\left(C_2 - 15\cos\beta + \cos 3\beta\right)\cos\beta\big] \end{aligned} \tag{69}$$

Since we are solving (68) on the sphere, we must ensure that P^∞ is not multiply-defined at the poles by enforcing that $P_1^\infty(\alpha,0)$ and $P_2^\infty(\alpha,\pi)$ must be independent of α and equal to each other (since the PDE is the same when rotated by an angle of π in β and has a unique solution). This can only be done by setting $C_1 = 10$ and $C_2 = 0$. P_1^∞ then simplifies to

$$P_1^\infty = \frac{1}{16\pi}\sin 2\alpha \sin^2\beta. \tag{70}$$

P_2^∞ can be calculated similarly, and is given by

$$P_2^\infty = -\frac{1}{30,270\pi}\left(19 + 60\cos 2\beta - 15\cos 4\beta + 120\cos 4\alpha \sin^4\beta\right). \tag{71}$$

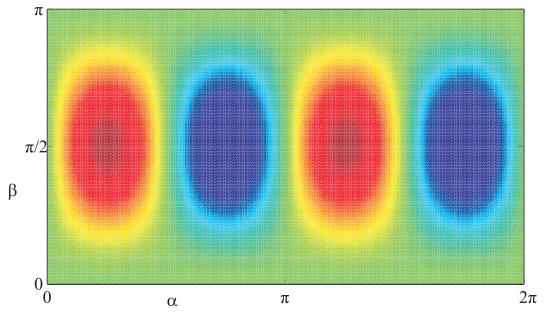

FIGURE 9. Plot of P^∞ for $\mu = \frac{\gamma B}{D} \ll 1$, given by equation (72) for $\mu = 0.1$ (left). Darker regions indicate the peaks and troughs. The peaks (red) are located at approximately $\alpha = \frac{\pi}{4}, \frac{5\pi}{4}$ with $\beta = \frac{\pi}{2}$.

Thus,

$$\begin{aligned} P^\infty =& \frac{1}{4\pi}\left[1 + \mu\frac{1}{4}\sin 2\alpha \sin^2\beta \right. \\ & \left. -\mu^2\frac{2}{15135}\left(19 + 60\cos 2\beta - 15\cos 4\beta + 120\cos 4\alpha \sin^4\beta\right)\right] \\ & + \mathcal{O}(\mu^3). \end{aligned} \tag{72}$$

A plot of P^∞ is given in Figure 9.

Using equation (29), we get the effective viscosity

$$\hat{\eta} := \frac{\Sigma_{12}}{\gamma} = \eta + \phi\left[\eta M_0 - \frac{f_p K}{160\pi a^2 \gamma}\mu + \eta M_2 \mu^2 + \mathcal{O}\left(\mu^3\right)\right] + \mathcal{O}(\phi^2), \tag{73}$$

where M_0 and M_2 are scalar functions of eccentricity e given by

$$M_0 := \frac{b^2}{a^2}\left(\frac{3}{5}\frac{(Y^H)^2}{Y^C} + \frac{1}{2}X^M + Y^M + Z^M\right) \tag{74a}$$

and

$$M_2 := -\frac{1}{420}\frac{b^2}{a^2}\left(\frac{3}{5}\frac{(Y^H)^2}{Y^C} - 2X^M + Y^M + Z^M\right), \tag{74b}$$

where Y^C, Y^H, X^M, Y^M, and Z^M are resistance functions defined in equations (93e-93i), and K is a scalar function of e and λ. M_i and K are plotted in Fig. 7 and 4, respectively. The second and fourth terms in equation (73) are the passive contributions due to the presence of inert spheroids. The third term is the active contribution due to forward self-propulsion. This formula indicates that the suspension is very weakly non-newtonian (since $\hat{\eta} = C + \mathcal{O}(\gamma^2)$). Once again, the active term does not disappear as $\gamma \to 0$. As before, this is a singular limit of the Fokker-Planck equation and we refer the reader to section 4.2 for further discussion.

Assuming $f_p > 0$, one can use equation (15a) to write equation (73) in terms of v.

The normal stress differences are given by

$$\frac{\Sigma_{11}-\Sigma_{22}}{\gamma^2} = 0 \tag{75}$$

$$\frac{\Sigma_{22}-\Sigma_{33}}{\gamma^2} = \left[\eta\frac{b^2}{7a^2\gamma}\left(\frac{3(Y^H)^2}{10Y^C}+\frac{X^M}{2}+\frac{Y^M}{2}-Z^M\right)\mu - \frac{f_pK}{2240\pi a^2\gamma^2}\mu + \mathcal{O}(\mu^2)\right]\phi + \mathcal{O}(\phi^2). \tag{76}$$

The results here, similar to those in section 4.1, contrast with those in [29] in that the first normal stress difference is zero. Nevertheless, as in [29], the active contribution to the second normal stress difference is negative for "pushers" ($f_p > 0$) and positive for "pullers" ($f_p < 0$).

4.4. **Effective viscosity in weak oscillatory flows.** We now place our particles in a pure oscillatory shear flow described by

$$E = \frac{1}{2}\sin\omega^0 t\begin{pmatrix} 0 & \gamma & 0\\ \gamma & 0 & 0\\ 0 & 0 & 0\end{pmatrix}, \tag{77}$$

$$\Omega = \left(0, 0, \frac{\gamma}{2}\sin\omega^0 t\right). \tag{78}$$

In this flow, the deterministic particle trajectories will obey

$$\begin{cases} \dot\alpha^D = \frac{\gamma}{2}\sin\omega^0 t\,(1+B\cos 2\alpha)\\ \dot\beta^D = \gamma\sin\omega^0 t\frac{B}{4}\sin 2\alpha\sin 2\beta. \end{cases} \tag{79}$$

Using these to construct $\dot{\hat{d}}$ and plugging them into (22) yields the time-dependent Fokker-Planck equation

$$\frac{\partial P}{\partial t} = \frac{1}{2}\gamma\sin\omega^0 t\left[B\sin 2\alpha\sin\beta\left(3P\sin\beta - \frac{\partial P}{\partial\beta}\cos\beta\right) - (1+B\cos 2\alpha)\frac{\partial P}{\partial\alpha}\right] + D\Delta_{\alpha,\beta}P. \tag{80}$$

Letting

$$L := B\sin 2\alpha\sin\beta\left(3\sin\beta - \cos\beta\frac{\partial}{\partial\beta}\right) - (1+B\cos 2\alpha)\frac{\partial}{\partial\alpha}, \tag{81}$$

writing

$$P(\alpha,\beta,t) = \sum_{k=-\infty}^{\infty} e^{ik\omega^0 t}P_k(\alpha,\beta), \tag{82}$$

and matching terms, we get

$$-k\omega P_k = \frac{\gamma}{4}\left(LP_{k-1} - LP_{k+1}\right) + iD\Delta_{\alpha,\beta}P_k. \tag{83}$$

Assuming $\gamma \ll D$, we can write $P_k = \sum_{l=0}^{\infty} P_{k,l}(\alpha,\beta)\left(\frac{\gamma}{D}\right)^l$ and get, for $P_{k,0}$,

$$-k\frac{\omega^0}{D}P_{k,0} = i\Delta_{\alpha,\beta}P_{k,0}. \tag{84}$$

These have solutions

$$P_{k,0} = \begin{cases} \frac{1}{4\pi} & k=0\\ 0 & k\neq 0. \end{cases} \tag{85}$$

In order to calculate the effective rheology, we only really need to know $P_{1,1}$ and $P_{-1,1}$, and we now have enough information to calculate them. Applying equation 83, we see that

$$\frac{\omega^0}{D}P_{-1,1} = -\frac{1}{4}L\frac{1}{4\pi} + i\Delta_{\alpha,\beta}P_{-1,1} \text{ and} \tag{86a}$$

$$-\frac{\omega^0}{D}P_{1,1} = \frac{1}{4}L\frac{1}{4\pi} + i\Delta_{\alpha,\beta}P_{1,1}. \tag{86b}$$

These have solutions

$$P_{-1,1} = \frac{3iBD}{16\pi(6D - i\omega^0)}\sin 2\alpha \sin^2\beta \text{ and} \tag{87a}$$

$$P_{1,1} = -\frac{3iBD}{16\pi(6D + i\omega^0)}\sin 2\alpha \sin^2\beta. \tag{87b}$$

Thus,

$$\begin{aligned} P_{-1}e^{-i\omega^0 t} + P_1 e^{i\omega^0 t} =& \frac{3}{8\pi}\frac{\gamma B \sin 2\alpha \sin^2\beta\left(6D\sin\omega^0 t - \omega^0\cos\omega^0 t\right)}{36D^2 + (\omega^0)^2} \\ &+ \mathcal{O}\left(\left(\frac{\gamma}{D}\right)^2\right). \end{aligned} \tag{88}$$

Using only the $\sin\omega^0 t$ portion of this, we get the effective viscosity

$$\begin{aligned} \hat{\eta} := \frac{\Sigma_{12}}{\gamma\sin\omega^0 t} =& \eta + \phi\left[\eta M_0 - K\frac{9Bf_pD}{40\pi a^2\left(36D^2 + (\omega^0)^2\right)} + \mathcal{O}\left(\frac{\gamma}{D}\right)\right] \\ &+ \mathcal{O}(\phi^2), \end{aligned} \tag{89}$$

where M_0 is a scalar function of eccentricity e given in equation (74a), and K is a scalar function of e and λ given in equation (42). M_0 and K are plotted in Fig. 7 and 4, respectively. Once again, the active term does not disappear as $\gamma \to 0$. As before, this is a singular limit of the Fokker-Planck equation and we refer the reader to section 4.2 for further discussion. Assuming $f_p > 0$, one can use equation (15a) to write equation (89) in terms of v.

The normal stress differences are given by

$$\frac{\Sigma_{11} - \Sigma_{22}}{\gamma^2\sin\omega^0 t} = 0 \tag{90}$$

$$\begin{aligned} \frac{\Sigma_{22} - \Sigma_{33}}{\gamma^2\sin\omega^0 t} =& \left[\eta\frac{18b^2BD}{35a^2\gamma(36D^2 + (\omega^0)^2)}\left(3\frac{(Y^H)^2}{Y^C} + 5\left(X^M + Y^M - 2Z^M\right)\right)\right. \\ &\left. + \mathcal{O}\left(\frac{\gamma}{D}\right)\right] + \mathcal{O}(\phi^2). \end{aligned} \tag{91}$$

It is notable that this is the only asymptotic result in which the normal stress differences contain no active contribution. However, the formulae for nearly-spherical particles in a steady shear flow (eq. (62)) imply that the active contribution should vanish for large $\frac{D}{\gamma}$, the limit in which this formula is valid.

4.5. **Numerics.** We now evaluate the Fokker Planck equations (67) and (59) numerically for bacteria in the flow described by

$$E = \frac{1}{2}\begin{pmatrix} 0 & \gamma & 0 \\ \gamma & 0 & 0 \\ 0 & 0 & 0 \end{pmatrix}, \tag{92}$$

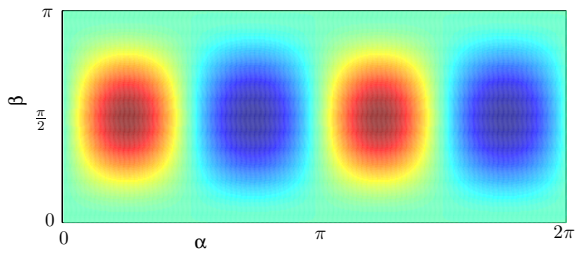

FIGURE 10. A plot of P^∞ in the flow without vorticity for $\gamma = 0.14s^{-1}$. Darker regions indicate the peaks and troughs. The peaks (red) are located at approximately $\alpha = \frac{\pi}{4}, \frac{5\pi}{4}$ with $\beta = \frac{\pi}{2}$.

with $\vec{\Omega} = (0,0,0)$ and $\vec{\Omega} = \left(0,0,\frac{\gamma}{2}\right)$, respectively. The numerics are performed using a finite difference scheme on a uniform mesh with 80,400 points with the resulting linear system solved using the method of biconjugate gradients. We then use these numerical solutions to evaluate $\frac{\hat{\eta}}{\eta} := \frac{\Sigma_{12}}{\eta\gamma}$ for a range of values of γ. We first perform these numerics for the case of elongated bacteria, allowing us to compare the results with the asymptotics in sections 4.1, 4.3, and 4.4. Next, we consider nearly spherical bacteria ($B \ll 1$) in order to compare the results with the asymptotics in section 4.2.

In the first case, we consider elongated bacteria with the various parameters set by values established in the literature. The results for the case of no vorticity ($\vec{\Omega} = (0,0,0)$) are plotted against γ in Fig. 5 along with asymptotics for small and large γ given in equations (73) and (52), respectively. The numerics are fit to $C_0 + C_1 \arctan\left(C_2\sqrt{(\gamma - C_3)^2 + C_4}\right)$ with $C_0 = -13930.70$, $C_1 = 8873.75$, $C_2 = 622.79$, $C_3 = 0.05$, and $C_4 = 2.87$. A plot of P^∞ in this case is given in Fig. 10 The results for the case with vorticity are plotted against γ in Fig. 6 along with asymptotics for small $\frac{\gamma}{D}$ given in equation (89). These numerics are fit to $C_0 + C_1 \arctan\left(C_2\sqrt{(\gamma - C_3)^2 + C_4}\right)$ with $C_0 = -7311.84$, $C_1 = 4661.12$, $C_2 = 845.92$, $C_3 = -0.03$ and $C_4 = 0.30$. A plot of P^∞ in this case is given in Fig. 11.

Next, we consdier the case of nearly spherical bacteria in the background flow without vorticity. We set $B := \frac{b^2-a^2}{b^2+a^2} = .01$ and all other parameters as above. A plot of P^∞ in this case is given in Figure 10. The results are plotted against γ in the inset to Fig. 6 along with asymptotics for small ϵ given in equation (61). A plot of P^∞ in this case is given in Fig. 11.

5. **Conclusions.** We have demonstrated that bacterial self-propulsion has the effect of decreasing the effective viscosity of an ambient fluid. For weak enough background flows, this decrease outweighs the increase in viscosity due to the fact that a bacterium is also a rigid particle to produce a net decrease in the viscosity of the fluid. Thus, qualitatively, the mechanism of decreased viscosity of bacterial suspensions in experiments can be explained without considering multi-body interactions. For strong background flows, as one expects, the effect of self-propulsion becomes negligible and an active suspension becomes indistinguishable from a passive suspension.

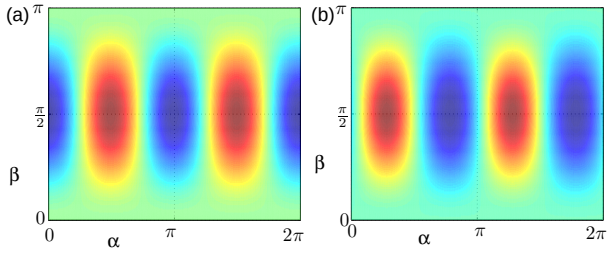

FIGURE 11. (a) A plot of P^∞ in the flow with vorticity for $B = \frac{b^2-a^2}{b^2+a^2} = .01$ and $\gamma = 0.017\text{s}^{-1}$. Darker regions indicate the peaks and troughs. The peaks (red) are located at approximately $\alpha = \frac{\pi}{2}, \frac{3\pi}{2}$ with $\beta = \frac{\pi}{2}$. (b) A plot of P^∞ in the flow with vorticity for $\frac{b}{a} = 5.7$ and $\gamma = 0.14s^{-1}$. Darker regions indicate the peaks and troughs. The peaks (red) are located at approximately $\alpha = \frac{\pi}{4}, \frac{5\pi}{4}$ with $\beta = \frac{\pi}{2}$.

The reduction in viscosity due to self-propulsion predicted in our model relies on the bacteria in question being "pushers" (i.e., $f_p > 0$). However, our results are still valid for "pullers" (e.g., some motile algae) which can be modeled in the same way but with $f_p < 0$. In this case, there is an increase in viscosity due to self propulsion. That there is a fundamental difference in the physics of "pushers" and "pullers" was previously observed in [14, 9].

Appendix A. **Resistance Functions.** This is a table of resistance functions for prolate spheroids taken from [21].

$$L = \log \frac{1+e}{1-e} \tag{93a}$$

$$X^A = \frac{8}{3}e^3 \left[-2e + \left(1+e^2\right) L\right]^{-1} \tag{93b}$$

$$Y^A = \frac{16}{3}e^3 \left[2e + \left(3e^2-1\right) L\right]^{-1} \tag{93c}$$

$$X^C = \frac{4}{3}e^3 \left(1-e^2\right) \left[2e - \left(1-e^2\right) L\right]^{-1} \tag{93d}$$

$$Y^C = \frac{4}{3}e^3 \left(2-e^2\right) \left[-2e + \left(1+e^2\right) L\right]^{-1} \tag{93e}$$

$$Y^H = \frac{4}{3}e^5 \left[-2e + (1+e^2)L\right]^{-1} \tag{93f}$$

$$X^M = \frac{8}{15}e^5 \left[(3-e^2)L - 6e\right]^{-1} \tag{93g}$$

$$\begin{aligned} Y^M =& \frac{4}{5}e^5 \left[2e(1-2e^2) - (1-e^2)L\right] \\ & \times \left[\left(2e(2e^2-3) + 3(1-e^2)L\right)\left(-2e + (1+e^2)L\right)\right]^{-1} \end{aligned} \tag{93h}$$

$$Z^M = \frac{16}{5}e^5(1-e^2) \left[3(1-e^2)^2 L - 2e(3-5e^2)\right]^{-1} \tag{93i}$$

Appendix B. **Existence, Uniqueness and Regularity results.** The existence and regularity of (8a) solutions cannot be established using the standard methods of functional analysis. This is because of the delta function in the right hand side of eq. (8a) which is *not* in H^{-1} – the standard Sobolev space for which results for elliptic PDEs are typically established. Furthermore, the fact that the domain of (8a) is unbounded necessitates the use of *homogeneous* Sobolev spaces (see, e.g., [8]) instead of these.

Thus, we analyze solvability by further decomposing problem 8a into two parts: $\vec{u}^d = \vec{u}^1 + \vec{u}^2$, where

$$\begin{cases} \Delta \vec{u}^1 = \eta \nabla p^1 + f_p \hat{d} \delta(\vec{x} - \vec{x}^f) & \vec{x} \in \Omega \setminus B \\ \nabla \cdot \vec{u}^1 = 0 & \vec{x} \in \Omega \setminus B \\ \vec{u}^1 = 0 & \vec{x} \in \partial B \\ \vec{u}^1 \to 0 & \vec{x} \to \infty \end{cases} \tag{94a}$$

and

$$\begin{cases} \Delta \vec{u}^2 = \eta \nabla p^2 & \vec{x} \in \Omega \setminus B \\ \nabla \cdot \vec{u}^2 = 0 & \vec{x} \in \Omega \setminus B \\ \vec{u}^2 = \vec{v} + \vec{\omega} \times (\vec{x} - \vec{x}^c) & \vec{x} \in \partial B \\ \vec{u}^2 \to E \cdot \vec{x} + \vec{\Omega} \times \vec{x} & \vec{x} \to \infty. \end{cases} \tag{94b}$$

The solution to equation (94a) is given by

$$\vec{u}^1 = f_p \hat{d} \cdot \frac{\mathcal{G}(\vec{x} - \vec{x}^c)}{8\pi\eta}, \quad p^1 = f_p \hat{d} \cdot \frac{\mathcal{P}(\vec{x} - \vec{x}^c)}{8\pi\eta}, \tag{95}$$

where $\mathcal{G}$ is the Oseen tensor, given by

$$\mathcal{G}_{ij} = \frac{1}{r}\delta_{ij} + \frac{1}{r^3} x_i x_j, \tag{96}$$

and $\mathcal{P}$ is its pressure field, given by

$$\mathcal{P}_i = 2\eta \frac{x_i}{r^3} + \mathcal{P}_i^\infty, \tag{97}$$

where $\mathcal{P}^\infty$ is constant but arbitrary. Problem (94b) is a standard Dirichlet problem with a solution (see, e.g., [8])

$$\vec{u}^2 \in D^{1,2}\left(\Omega \setminus B\left(\vec{x}^c, \hat{d}\right)\right), \quad p^2 \in L^2\left(\Omega \setminus B\left(\vec{x}^c, \hat{d}\right)\right), \tag{98}$$

where $D^{1,2}(\Omega)$ is a homogeneous Sobolev space defined by

$$D^{1,2}(\Omega) := \left\{ f : f \in L^1_{\text{loc}}(\Omega), \sum_{|\alpha|=1} \|f^{(\alpha)}\|_{L^2(\Omega)} < \infty \right\}. \tag{99}$$

Thus, the full solution is the sum of $(\vec{u}^1, p^1)$ and $(\vec{u}^2, p^2)$ and, therefore, lies in an affine space of functions parameterized by the location and the orientation of the bacterium:

$$\vec{u} \in \mathcal{A}^u\left(\vec{x}^c, \hat{d}\right) := D^{1,2}\left(\Omega \setminus B\left(\vec{x}^c, \hat{d}\right)\right) + c\hat{d} \cdot \frac{\mathcal{G}(\vec{x} - \vec{x}^c)}{8\pi\eta} \tag{100}$$

and

$$p \in \mathcal{A}^p\left(\vec{x}^c, \hat{d}\right) := L^2\left(\Omega \setminus B\left(\vec{x}^c, \hat{d}\right)\right) + c\hat{d} \cdot \frac{\mathcal{P}(\vec{x} - \vec{x}^c)}{8\pi\eta}. \tag{101}$$

REFERENCES

[1] G. Batchelor. The stress system in a suspension of force-free particles. *J. Fluid Mech.*, 41(3):545–570, 1970.

[2] G. K. Batchelor and J. T. Green. The determination of the bulk stress in a suspension of spherical particles to order c^2. *J. Fluid Mech.*, 56:401–427, 1972.

[3] L. Berlyand, L. Borcea, and A. Panchenko. Network approximation for effective viscosity of concentrated suspensions with complex geometry. *SIAM J. Math. Anal.*, 36(5):1580–1628, 2005.

[4] L. Berlyand, Y. Gorb, and A. Novikov. Fictitious fluid approach and anomalous blow-up of the dissipation rate in a 2d model of concentrated suspensions. *Arch. Rat. Mech. Anal.*, 2008.

[5] L. Berlyand and A. Panchenko. Strong and weak blow up of the viscous dissipation rates for concentrated suspensions. *J. Fluid Mech.*, 578:1–34, 2007.

[6] H. Brenner and D. W. Condiff. Transport mechanics in systems of orientable particles: Iii. arbitrary particles. *J. Colloid and Interface Sci.*, 41(2):228–274, 1972.

[7] A. Einstein. *Investigations on the theory of the Brownian movement*. Dover Publications, New York, 1956.

[8] G. P. Galdi. *An Introduction to the Mathematical Theory of the Navier-Stokes Equations, Vol. I*. Springer, New York, 1994.

[9] V. T. Gyrya, I. S. Aranson, L. V. Berlyand, and D. A. Karpeev. A model of hydrodynamic interaction between swimming bacteria. *Bull. Math. Biol.*, 2009.

[10] B. M. Haines. Justification of einstein's effective viscosity result. in preparation.

[11] B. M. Haines, I. S. Aranson, L. Berlyand, and D. A. Karpeev. Effective viscosity of dilute bacterial suspensions: a two-dimensional model. *Phys. Biol.*, 5, 2008.

[12] B. M. Haines, A. Sokolov, I. S. Aranson, L. Berlyand, and D. A. Karpeev. A three-dimensional model for the effective viscosity of bacterial suspensions. *Phys. Rev. E*, 80:041922, 2009.

[13] Y. Hatwalne, S. Ramaswamy, M. Rao, and R. A. Simha. Rheology of active-particle suspensions. *Phys. Rev. Lett.*, 92:118101, 2004.

[14] J. P. Hernandez-Ortiz, C. G. Stoltz, and M. D. Graham. Transport and collective dynamics in suspensions of confined swimming particles. *Phys. Rev. Lett.*, 95:204501, 2005.

[15] E. J. Hinch and L. G. Leal. The effect of brownian motion on the rheological properties of a suspension of non-spherical particles. *J. Fluid Mech.*, 52(4):683–712, 1972.

[16] T. Ishikawa and T. J. Pedley. The rheology of a semi-dilute suspension of swimming model micro-organisms. *J. Fluid Mech.*, 588:399, 2007.

[17] K. Ito. Stochastic integral. *Proc. Imperial Acad., Tokyo*, 20:519–524, 1944.

[18] K. Ito. On stochastic differential equations on a differentiable manifold 2. *mem. Coll. Sci. Kyôto Univ.*, 28:82–85, 1953.

[19] G. B. Jeffery. The motion of ellipsoidal particles immersed in a viscous fluid. *R. Soc. London Ser. A*, 102:161–79, 1922.

[20] M. J. Kim and K. S. Breuer. Use of bacterial carpets to enhance mixing in microfluidic systems. *Jour. Fluids Engin.*, 129(319), 2007.

[21] S. Kim and S. Karrila. *Microhydrodynamics*. Dover Publications, New York, 1991.

[22] L. G. Leal and E. J. Hinch. The effect of weak brownian rotations on particles in shear flow. *J. Fluid Mech.*, 46(4):685–703, 1971.

[23] T. Levy and E. Sanchez-Palencia. Suspension of solid particles in a newtonian fluid. *J. Non-Newt. Fluid Mech.*, 13:63–78, 1983.

[24] R. M. Macnab. The bacterial flagellum: Reversible rotary propellor and type iii export apparatus. *J. Bacteriology*, 181(23):7149–7153, 1999.

[25] H. P. McKean. *Stochastic Integrals*. Academic Press, New York and London, 1969.

[26] K. C. Nunan and J. B. Keller. Effective viscosity of a periodic suspension. *J. Fluid Mech.*, 142:269–287, 1984.

[27] T. J. Pedley and J. O. Kessler A new continuum model for suspensions of gyrotactic micro-organisms. *J. Fluid Mech.*, 212:155–182, 1990.

[28] H. Risken. *The Fokker-Planck Equation: Methods of Solution and Applications*. Springer-Verlag, New York, 1989.

[29] D. Saintillan. The dilute rheology of swimming suspensions: A simple kinetic model. *Experimental Mechanics*.

[30] J. Shioi, S. Matsuura, and Y. Imae. Quantitative Measurements of Proton Motive Force and Motility in Bacillus Subtilis. *J. Bacteriol.*, 144(3):891–897, 1980.

[31] A. Sokolov and I. S. Aranson. Reduction of viscosity in suspension of swimming bacteria. *Phys. Rev. Lett.*, 103(14):148101, 2009.

[32] A. Sokolov, I. S. Aranson, J. O. Kessler, and R. E. Goldstein. Concentration dependence of the collective dynamics of swimming bacteria. *Phys. Rev. Lett.*, 98:158102, 2007.

[33] A. Sokolov, R. E. Goldstein, F. I. Feldchtein, and I. S. Aranson. Enhanced mixing and spatial instability in concentrated bacterial suspensions. *Phys. Rev. E*, 80:031903, 2009.

[34] G. Subramanian and D. L. Koch. Critical bacterial concentration for the onset of collective swimming. *J. Fluid Mech.*, 632:359–400, 2009.

[35] L. Turner, W. S. Ryu, and H. C. Berg. Real-time imaging of fluorescent flagellar filaments. *J. Bacteriol.*, 182:2793–2801, 2000.

[36] I. Tuval, L. Cisneros, C. Dombrowski, C. W. Wolgemuth, J. O. Kessler, and R. E. Goldstein. Bacterial swimming and oxygen transport near contact lines. *PNAS*, 102(7):2277–2282, 2005.

[37] M. Wu, J. W. Roberts, S. Kim, D. L. Koch, and M. P. Delisa. Collective bacterial dynamics revealed using a three-dimensional population-scale defocused particle tracking technique. *Applied and Environmental Microbiology*, 72(7):4987–4994, 2006.

[38] X.-L. Wu and A. Libchaber. Particle diffusion in a quasi-two-dimensional bacterial bath. *Phys. Rev. Lett.*, 84:3017, 2000.

E-mail address: haines@math.psu.edu
E-mail address: aronson@anl.gov
E-mail address: berlyand@math.psu.edu
E-mail address: karpeev@mcs.anl.gov